

P.32

National Aeronautics and Space Administration

IUE OBSERVING PROGRAM
FINAL TECHNICAL REPORT FOR NAG 5-1425

Submitted to:

Dr. Y. Kondo
Code 684
Laboratory for Astronomy & Solar Physics
Space and Earth Sciences Directorate
Goddard Space Flight Center
Greenbelt, MD 20771

Submitted by:

The Trustees of Columbia University
in the City of New York
Box 20, Low Memorial Library
New York, New York 10027

Prepared by:

Columbia Astrophysics Laboratory
Departments of Astronomy and Physics
Columbia University
538 West 120th Street
New York, New York 10027

Title of Research:

**IUE and ROSAT Monitoring of the
Bright QSO H1821+643**

Principal Investigator:

Jules Halpern
Associate Professor of Physics

Co-Investigators:

Michiel Kolman
Chris Shrader
Alexei Filippenko

Period Covered by Report:

1 September 1990 - 31 August 1991

(NASA-CR-188719) IUE AND ROSAT MONITORING
OF THE BRIGHT QSO H1821+643 Final Technical
Report, 1 Sep. 1990 - 31 Aug. 1991
(Columbia Univ.) 32 p

N91-31029

CSCL 03A

Unclass

63/89 0032972

TABLE OF CONTENTS

1. Summary	1
2. Introduction	2
3. Ultraviolet Observations	3
3.1. Short-term UV Variability	4
3.2. Long-term UV Variability	5
3.3. Emission Lines	5
3.4. Absorption Lines	6
4. Optical Observations	7
Tables	9
References	12
Figure Captions	13
Figures	14
Appendix: Papers Published Under NASA Grant NAG 5-1425	18

IUE and ROSAT Monitoring of the Bright QSO H1821+643

Final Technical Report

1. SUMMARY

We report on the analysis of *IUE* observations of the bright QSO H1821+643, obtained during the *ROSAT* All Sky Survey (the *RIASS* program). This grant funded the research of the "US Principal Investigator" on this particular target. The aims of this investigation were 1) to establish whether the UV and soft X-ray radiation have the same physical origin, and 2) to determine if this physical origin is an accretion disk. The chosen target was uniquely suited to this investigation, as it is both very bright, and fortuitously located near the north ecliptic pole where it was continuously visible to the *ROSAT* PSPC for ~ 35 days. Supporting ground-based spectrophotometry was also obtained. Our analysis shows that the shape and flux level of the UV continuum did not vary among the seven *IUE* observations spanning one month, to an upper limit of about 8%. So it is of great interest to determine whether the soft X-ray flux varied during this period. Since X-ray variability in AGNs is often more rapid and of higher amplitude than in the UV, detection of X-ray variability in the *ROSAT* data could severely challenge the accretion disk model for the soft X-ray excess. But unfortunately, the *ROSAT* survey data are not yet available for study.

Analysis of this and previous *IUE* data on H1821+643 yield the following additional results:

1. Variations of 20% in continuum flux over time scales of months to years, accompanied by changes in spectral slope.
2. Constancy of the emission-line fluxes over the same period.
3. Measurements of Galactic absorption lines, and candidate low-redshift Lyman α forest lines, as have recently been detected in the spectrum of 3C 273 by *HST*.

2. INTRODUCTION

The bright ($V=14.2$ mag) QSO H1821+643 has been observed extensively during the last few years. In Kolman, Halpern, Shrader, and Filippenko (1991, hereafter KHSF, see Appendix) we reported on the first *IUE* observations of this QSO and its overall continuum energy distribution. H1821+643 displayed a strong optical/UV bump and a similarly strong, variable soft X-ray excess. This object is also one of the brightest QSOs observed by hard X-ray instruments, and by *IRAS*. It is quiet only at radio wavelengths. Optical imaging showed that H1821+643 is located in a group of galaxies (Hutchings and Neff 1991).

The intermediate redshift of H1821+643 ($z = 0.297$) makes it well suited to a study of the intrinsic ultraviolet continuum, as higher redshift objects suffer from absorption by intergalactic HI clouds. Moreover, its location only 3° from the ecliptic pole made H1821+643 an important object for monitoring with *IUE* during the *ROSAT* All Sky Survey, as it was visible to the *ROSAT* PSPC for ~ 35 days. Considering the strong and variable emission detected in the UV and at soft X-ray energies (KHSF 1991), this is an ideal object to test for a common origin of the UV big bump and the soft X-ray excess, an association which has yet to be proven. By determining the time scale of the variability and the correlation between the UV and soft X-ray emission, we might be able to establish that both arise in the inner disk, where the dynamical time is expected to be ~ 10 days. The reported minimum doubling time of about 10 days at X-ray energies (Snyder and Wood 1984) is consistent with t_{dyn} , defined as $t_{\text{dyn}} = (1+z) R_{\text{max}}/v_{\text{max}}$, where R_{max} is the radius at which the temperature of the disk reaches a maximum ($R_{\text{max}} \sim 8GM/c^2$), and $v_{\text{max}} = (GM/R_{\text{max}})^{1/2}$. Thus, $t_{\text{dyn}} \sim 1.7(M/10^9 M_\odot)$ days. Fits to the continuum spectrum indicate $M \sim 3 \times 10^9 M_\odot$ (KHSF), so the relevant time scales are well sampled during the 35 day *ROSAT* visibility window.

In this report, we describe the results of the ultraviolet spectroscopy which we obtained with *IUE* during the *ROSAT* All Sky Survey. Unfortunately, at the time of writing

(August 1991), the *ROSAT* data have not yet been made available to us as stipulated by the *RIASS* agreement, so the most interesting question still cannot be addressed. Problems in the production of the survey data are still being encountered by the *ROSAT* team. But we will incorporate the X-ray data into our analysis as soon as they are released to us, and a future paper will report the results.

3. ULTRAVIOLET OBSERVATIONS

All the new *IUE* observations are listed in Table 1. Seven pairs of images were obtained, approximately every 5 days from mid-October to mid-November 1990, during the period of maximum *ROSAT* exposure. The images were obtained with the large aperture in the low dispersion mode, resulting in a spectral resolution of $\sim 5 \text{ \AA}$ and $\sim 8 \text{ \AA}$ for the SWP and LWP, respectively. The spectra were obtained from the line-by-line images with the Gaussian extraction routines (at the Goddard Regional Data Analysis Facility) to minimize the noise while maintaining accurate flux levels. Both the SWP and LWP data are corrected for the slight temperature dependency of the detector sensitivity. The LWP data were calibrated with the standards obtained in 1984-1985 (Cassatella, Lloyd, & Riestra 1988). The May 1980 flux calibration was used for the SWP data. The accuracy of this calibration is estimated at $\sim 10\%$ (Bohlin & Holm 1980), but work by Finley et al. (1990) suggests that the actual calibration could be up to 20% different from the May 1980 calibration.

We corrected the spectra for the effects of interstellar reddening, using the extinction curve of Seaton (1979) and $E(B - V) = 0.085 \text{ mag}$. The color excess is based on the neutral hydrogen column density in the direction of H1821+643 ($N_{\text{H}} = 4.1 \times 10^{20} \text{ cm}^{-2}$, Stark et al. 1991) and the $N_{\text{H}}/E(B - V)$ ratio of $4.8 \times 10^{21} \text{ cm}^{-2} \text{ mag}^{-1}$ (Bohlin, Savage, and Drake 1978). We did not correct for any internal reddening, as the intrinsic extinction in luminous QSOs is thought to be generally small (Sun and Malkan 1989, and references therein). We flagged the data points due to saturation, cosmic ray hits, or the presence

of reseaux. The coadded spectrum is shown in Figure 1. Despite the decline in sensitivity below 1200 Å, there is strong emission shortward of the Lyman limit (which is redshifted to 1182 Å), similar to the result reported in KHSF (1991).

3.1. Short-term UV Variability

The seven SWP and LWP spectra are all shown in Figure 2. The continuum was studied for variability by testing a number of continuum points against their time-averaged averaged flux $\langle f \rangle$ (shown in Figure 3 as the dashed lines and listed in Table 2). The error bars shown are the rms standard deviation from the mean in each continuum interval i , namely $\sigma_i = \left[\sum_{j=1}^N (f_j - \langle f \rangle)^2 / (N - 1) \right]^{1/2}$, where N is the number of points comprising the continuum interval. These errors might underestimate the true error as the uncertainty in the calibration is not taken into account. This is especially important below 1200 Å. The exact errors of the *IUE* are not known. In Table 2, the second column gives the (error weighted) average flux $\langle f \rangle = \left(\sum_{i=1}^7 f_i / \sigma_i^2 \right) / \left(\sum_{i=1}^7 1 / \sigma_i^2 \right)$, the third column $\chi^2 = \sum_{i=1}^7 [(f_i - \langle f \rangle) / \sigma_i]^2$, and the fourth column the goodness-of-fit probability (where $q = 1$ corresponds to a perfect fit and $q \sim 10^{-2}$ or less to significant variability). Constancy of flux at all continuum wavelength intervals can be inferred, as the large q values listed in Table 2 demonstrate. The last column in Table 2 gives the upper limits to the variability as a percentage of the average flux. These upper limits are conservatively estimated from the 1σ error estimates on the fluxes. At the wavelengths of highest detector sensitivity (around 1890 Å and 2700 Å), the maximum variation is certainly less than 8% of the flux level on a time scale of one to four weeks. In summary, neither the continuum level nor the spectral shape was found to vary during the one month monitoring with *IUE*.

The ratio of flux shortward and longward of the Lyman limit (redshifted to 1182 Å) did not vary significantly from the average (0.88 ± 0.13 , where the error is the uncertainty in the flux ratio based on the σ 's of the flux from the 1164-1182 Å and 1231-1254 Å continuum bins), implying a constant covering fraction of $12 \pm 13\%$. A similar analysis

for the coadded spectrum obtained in 1987 and 1989, yields a slightly smaller, but not statistically different covering fraction of $5 \pm 10\%$.

3.2. Long-term UV Variability

KHSF discussed three sets of SWP and LWP spectra taken in 1987, and in February and June of 1989. These data can be compared with the coadded spectrum obtained in October and November 1990 to study the long-term variability in the UV continuum. As shown in Figure 4, neither the flux level nor the spectral shape changed between July 1987 and February 1989. But the June 1989 observation changed significantly in spectral shape, as it was considerably harder. The 1990 data showed the same spectral shape as found in 1987 and early 1989, but the overall flux level was 20% lower.

The sensitivity of the *IUE* detectors is known to degrade with time and we did not correct for this in our data reduction. For the LWP the change in sensitivity was (in the period 1985-1989) at most $\sim 1\%$ per year (Teays & Garhart 1990). The SWP sensitivity decreased rapidly prior to 1980, but the most recent measurements (from 1984-1986, Bohlin & Grillmair 1988) showed variations similar to the LWP (except at higher wavelengths: $\sim 2\%$ per year around 1950 \AA). Therefore, we estimate that the contribution of the detector degradation to the change in flux level is at most $\sim 2\%$ out of the total of 20% between 1989 and 1990.

To investigate the significance of the variations, the four data points were fitted with the (error weighted) average flux (indicated by the dashed line in Figure 3). The goodness-of-fit probability q is listed in Table 3, together with the average flux and χ^2 . The continuum points around 1890 \AA were most significantly variable, with $q = 1.3 \times 10^{-8}$.

3.3. Emission Lines

Information on continuum emission in the unobservable EUV gap can be derived from the UV and optical emission lines, which are powered by photons with EUV energies.

To this end, we measured the major emission lines in the UV and optical spectra. No significant differences in line fluxes were found from one *IUE* observation to the other in 1990; therefore, all the *IUE* spectra were coadded and dereddened. The measured line properties are listed in Table 4 and the lines are identified in Figure 1. The Ly α emission line could not be measured, as all spectra were saturated at this line (deliberately, in order to optimize the exposure in the continuum). In Table 4 we list the formal errors, where the error relative to the flux in the individual line emission data point is approximated by the relative σ in the continuum bins bordering the emission line. As often is the case, the major source of error in the line measurements is the uncertainty in the placement of the continuum, which can be contaminated by the broad wings of the emission lines, Galactic absorption lines, and blended Fe II line and Balmer continuum emission. Therefore, the formal error seriously underestimates the actual error in the line measurements.

For the O VI $\lambda 1034$ emission line, only the narrow component was measured (with full width at zero intensity, FWZI, of ~ 40 Å), as it was unclear how far the broad wings extend (possibly from 1260 Å to ~ 1400 Å, encompassing the Galactic absorption feature around 1300 Å). This uncertainty around the O VI line also complicates the measurement of the upper limit to C III $\lambda 977$ at its redshifted wavelength of 1267 Å, as well as the measurement of the O I $\lambda 1302$, Si II $\lambda 1304$ absorption feature.

The UV line fluxes in 1990 can be compared to the ones obtained in 1987 and 1989. The flux measurements stayed within the formal error range and, therefore, did certainly not change significantly. The equivalent widths increased on average by $\sim 20\%$ in 1990, which can be completely accounted for by the lower overall continuum level at that time.

3.4. Absorption Lines

We measured the absorption lines listed in Table 5. The lines are from low-ionization species, except for C IV for which only an upper limit is obtained due to its location on the blue wing of Ly α . Compared to the measurements of KHSF, the equivalent widths

are smaller, especially true for the various Fe II lines, which fall in the low-sensitivity part of the LWP camera. Since the present coadded spectrum has much better signal-to-noise, the newer measurements are to be preferred.

In H1821+643, the spectral region between Lyman α and C IV $\lambda 1549$ covers the redshift range 0.04 – 0.27 for detection of C IV absorption lines arising between the QSO and the Galaxy. In this sensitive part of the SWP camera, no such absorption features were found above the detection threshold of $EW \sim 0.2 \text{ \AA}$. The spectral region shortward of the Lyman α emission line allows the detection of low-redshift Lyman α forest lines. In the coadded spectrum of 1987 and 1989 we detected two absorption features around 1470 and 1490 \AA (with $EW = 0.7 \pm 0.2 \text{ \AA}$ and $1.0 \pm 0.2 \text{ \AA}$, respectively, the errors being formal), which could have been attributed to intergalactic Lyman α . In the coadded data obtained in 1990, we only detected the 1490 \AA feature ($EW = 0.6 \pm 0.2 \text{ \AA}$). In comparison, *HST* has detected 14 Lyman α forest lines in the redshift range 0.016–0.151 in the spectrum of 3C 273 (Morris et al. 1991; Bahcall et al. 1991). This surprising result indicates a flattening of the evolution of the absorbers, so that the comoving number density is roughly constant between $z = 2$ and $z = 0$. Two of the lines in 3C 273 have equivalent widths of $\sim 0.3 \text{ \AA}$ (Morris et al. 1991), so it is reasonable to expect that 1 or 2 Ly α lines may be just detectable in our higher redshift QSO. The final *IUE* archive, which will incorporate fixed pattern-noise removal, will enhance the detectability of these absorption lines in our coadded spectra. And observations with greater spectral resolution and sensitivity, i.e., with *HST*, will undoubtedly establish several detections of Ly α absorption lines in H1821+643.

4. OPTICAL OBSERVATIONS

Alex Filippenko has been monitoring H1821+643 since 1987 with spectrophotometry obtained at Lick Observatory. (The optical observing was not supported by this grant). Spectra were obtained approximately once per month in the period immediately preceding,

and during the *IUE* and *ROSAT* observations. A log of the most recent observations is shown in Table 6. The UV Schmidt spectrograph (Miller and Stone 1987) at the Cassegrain focus of the Shane 3-m reflector was used with a wide slit ($6-10''$, depending on seeing and moonlight) to obtain an accurate measurement of the flux. Usually, the entire "optical" wavelength range of 3100–9900 Å was covered, so that continuous spectra of the entire optical/UV big bump have been obtained.

Conditions were photometric most of the time, but even spectra obtained under non-photometric conditions will be useful for this monitoring project, because the constant [O III] lines which are relatively strong in this QSO can be used to rescale the flux. With regard to the variability of the UV big bump, KHSF noted that this feature extends to an observed wavelength of $1\ \mu\text{m}$ in H1821+643, so the optical spectra will be of great value in detecting small-amplitude variations, or in setting upper limits more stringent than the *IUE* limits. Reduction of the optical spectra (not supported by this grant) is still in progress, and they will be incorporated into the analysis when the *ROSAT* X-ray data become available.

TABLE 1
IUE OBSERVATIONS OF H1821+643

Image	Int. time (min.)	Date
SWP 39826	290	1990 Oct 13
LWP 19005	123	1990 Oct 13
SWP 39868	270	1990 Oct 19
LWP 19035	108	1990 Oct 19
SWP 39930	290	1990 Oct 23
LWP 19054	120	1990 Oct 23
SWP 39985	279	1990 Oct 28
LWP 19085	120	1990 Oct 28
SWP 40046	280	1990 Nov 4
LWP 19144	106	1990 Nov 4
SWP 40089	272	1990 Nov 9
LWP 19182	100	1990 Nov 9
SWP 40103	271	1990 Nov 13
LWP 19219	100	1990 Nov 13

TABLE 2
SHORT-TERM UV VARIABILITY
(1990 October - November)

λ (Å)	$\langle f \rangle$ (mJy)	χ^2	q	variability ^a (% of $\langle f \rangle$)
1155-1190	2.45	0.53	.997	38
1230-1250	2.82	0.54	.997	20
1420-1495	3.59	0.69	.995	13
1715-1790	4.63	3.11	.795	10
1865-1915	4.64	2.32	.888	8
2610-2780	6.50	0.72	.994	8
2815-3000	7.12	1.27	.973	11
α^b	0.95 ^b	1.80	.937	11

^a upper limit on the variability relative to $\langle f \rangle$

^b power law index of the *IUE* (SWP+LWP) continuum fit ($F_\nu \propto \nu^{-\alpha}$).

TABLE 3
LONG-TERM UV VARIABILITY
(1987 - 1990)

λ (Å)	$\langle f \rangle$ (mJy)	χ^2	q
1155-1190	2.94	5.5	1.4×10^{-1}
1230-1250	3.33	20.4	1.4×10^{-4}
1420-1495	4.04	12.2	6.7×10^{-3}
1715-1790	5.30	20.9	1.1×10^{-4}
1865-1915	5.26	39.6	1.3×10^{-8}
2610-2780	6.99	25.6	1.1×10^{-5}
2815-3000	7.72	17.9	4.6×10^{-4}
α^a	0.95^a	10.3	1.6×10^{-2}

^a power law index of the *IUE* (SWP+LWP) continuum fit ($F_\nu \propto \nu^{-\alpha}$).

TABLE 4
EMISSION-LINE MEASUREMENTS OF H1821+643

ID ^a	Intensity ^b	Flux ^c	EW ^d
C III λ 977	$<4.1 \pm 0.3$	$<2.4 \pm 0.2$	$<7.5 \pm 0.4$
O VI λ 1034 ^e	13.0 ± 0.5	7.9 ± 0.3	20.4 ± 1.0
Si IV λ 1397, O IV λ 1407	5.0 ± 0.2	3.3 ± 0.1	11.8 ± 0.4
C IV λ 1549	52.0 ± 3.5	31.5 ± 2.1	$145. \pm 23.$
He II λ 1640, (O III] λ 1663)	14.1 ± 1.2	8.0 ± 0.7	40.9 ± 4.8
C III] λ 1909	9.8 ± 0.3	6.6 ± 0.2	32.4 ± 1.3

^a Identification of emission line and rest wavelength; the lines in parentheses denote only minor contributions.

^b Intensity corrected for Galactic reddening, in 10^{-13} ergs cm⁻² s⁻¹.

^c Observed flux in 10^{-13} ergs cm⁻² s⁻¹.

^d Observed equivalent width in Å.

^e Narrow component only (FWZI ~ 40 Å).

TABLE 5
ABSORPTION-LINE MEASUREMENTS OF H1821+643

ID	EW (Å)
S II λ 1251, 1254, 1260, Si II λ 1260	0.8 ± 0.2
O I λ 1302, Si II λ 1304	1.8 ± 0.2
C IV λ 1548,51	$<0.8 \pm 0.2$
Al II λ 1671	1.3 ± 0.2
Fe II λ 2343	0.8 ± 0.4
Fe II λ 2374,2382	1.6 ± 0.2
Fe II λ 2586	1.3 ± 0.2
Fe II λ 2599	1.8 ± 0.2
Mg II λ 2796,2803	3.6 ± 0.2

TABLE 6
OPTICAL OBSERVATIONS

U.T. Date	Wavelength (Å)	Res. (Å)
1988 Sep 18	3100–9990	13–16
1988 Oct 3	3100–9990	12–14
1989 Mar 29	3100–8900	12–14
1989 Jul 9	3100–8900	12–14
1990 Mar 25	3900–7100	12–14
1990 Apr 1	3900–7100	12–14
1990 May 1	3400–9800	6–14
1990 Jul 30	3100–9900	6–14
1990 Aug 30	3100–9900	6–14
1990 Sep 27	3900–9900	12–14
1990 Oct 20	3100–9900	6–14
1990 Nov 11	3100–9900	6–14
1991 Jul 20	3100–9900	12–14
1991 Aug 4	3100–9900	6–14

REFERENCES

- Bachall, J. N., Jannuzi, B. T., Schneider, D. P., Hartig, G. F., Bohlin, R., & Junkharinen, V. 1991, *Ap. J. (Letters)*, in press.
- Bohlin, R. C., & Grillmair, C. J. 1988, *Ap. J. Suppl.*, **66**, 209.
- Bohlin, R. C., & Holm, A. V. 1980, in NASA *IUE* Newsletter No. 10, p. 37.
- Bohlin, R. C., Savage, B. D., & Drake, J. F. 1978, *Ap. J.*, **224**, 132.
- Cassatella, A., Lloyd, C., & Riestra, R. G. 1988, in NASA *IUE* Newsletter No. 35, p. 225.
- Finley, D. S., Basri, G., & Bowyer, S. 1990, *Ap. J.*, **359**, 483.
- Hutchings, J. B., & Neff, S. G. 1991, *A. J.*, **101**, 434.
- Kolman, M., Halpern, J. P., Shrader, C. R., & Filippenko, A. V. 1991, *Ap. J.*, **373**, 57.
- Miller, J., and Stone, R. 1987, *Lick Observatory Technical Report No. 48*.
- Morris, S. L., Weymann, R. J., Savage, B. D., & Gilliland, R. L. 1991, *Ap. J. (Letters)*, in press.
- Seaton, M. J. 1979, *M.N.R.A.S.*, **187**, 73P.
- Snyder, W. A., and Wood, K. S. 1984, in *X-ray and UV Emission from Active Galactic Nuclei*, ed. W. Brinkman and J. Truemper (Garching), p. 114.
- Stark, A. A., Heiles, C., Bally, J., & Linke, R. 1991, in preparation.
- Sun, W.-H., & Malkan, M. A. 1989, *Ap. J.*, **346**, 68.
- Teays, T. J. & Garhart, M. P. 1990, in NASA *IUE* Newsletter No. 41, p. 94.

FIGURE CAPTIONS

FIG. 1. – Coadded spectrum of H1821+643 obtained with *IUE* in 1990, corrected for the estimated interstellar extinction of $E(B - V) = 0.085$ mag. Data points are flagged (X's) due to cosmic ray hits and the presence of reseaux. The $\text{Ly}\alpha$ emission is flagged due to saturation. Note the strong flux below the Lyman limit at 1182 Å.

FIG. 2. – Individual spectra of H1821+643 obtained in 1990, before dereddening. Flagged data points are deleted. The spectra are displayed chronologically, with the first at the bottom and last at the top. The SWP and LWP spectra are offset by 3 and 7 mJy, respectively. Note the lack of significant changes from one spectrum to another.

FIG. 3. – Test for short-term variability of the ultraviolet continuum emission for the spectra obtained in 1990 October and November. The dashed line indicates the error-weighted average flux (listed in Table 2). Note the absence of significant variations for all wavelengths, as well as the power law index.

FIG. 4. – Test for long-term variability of the ultraviolet continuum emission for the spectra obtained between 1987 and 1990. The dashed line indicates the error-weighted average flux (listed in Table 3). Note the absence of change between 1987 and early 1989, and the significant change in spectral shape during 1989. The 1990 continuum flux is consistently lower than the previous observations, while the spectral shape does not differ significantly from the 1987 and early 1989 spectra.

Figure 1

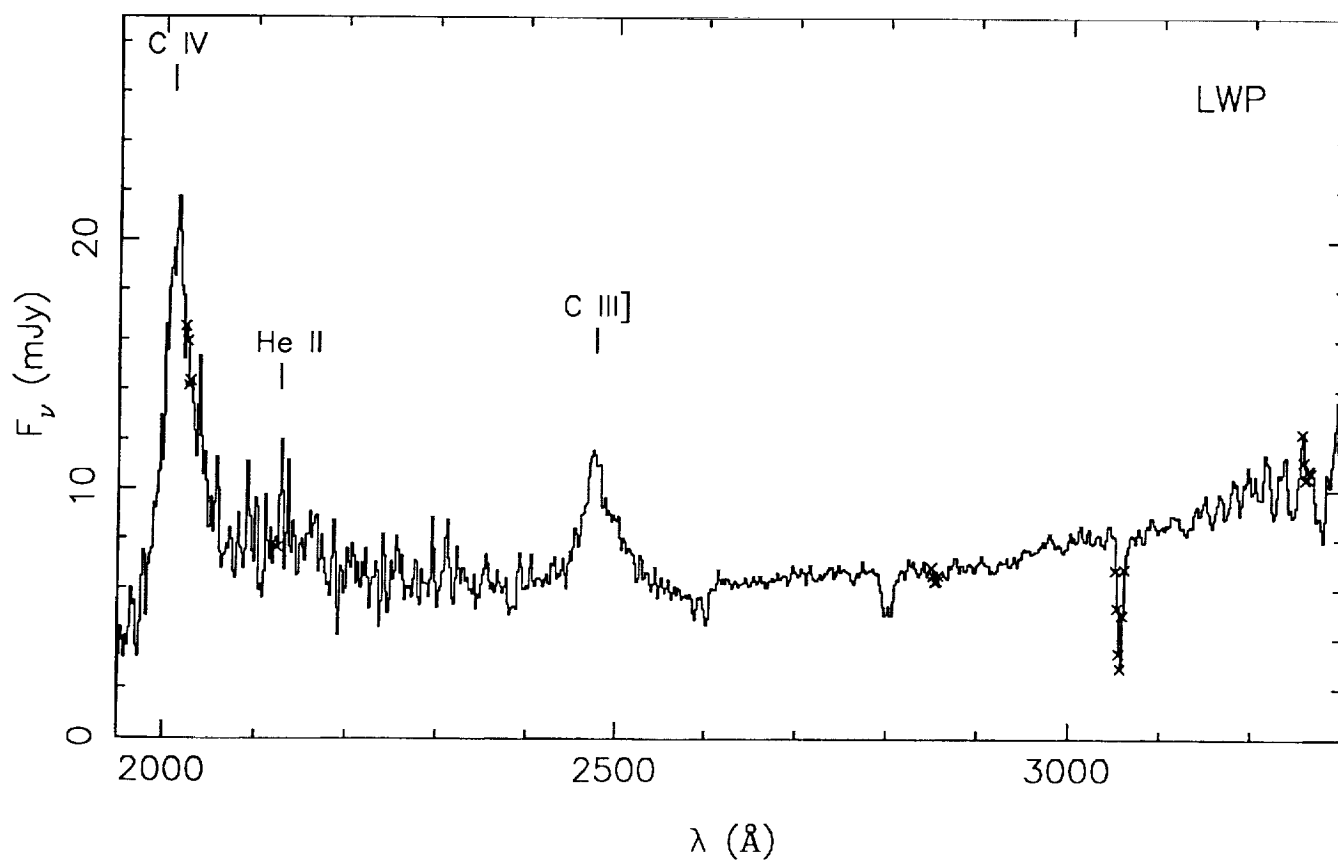
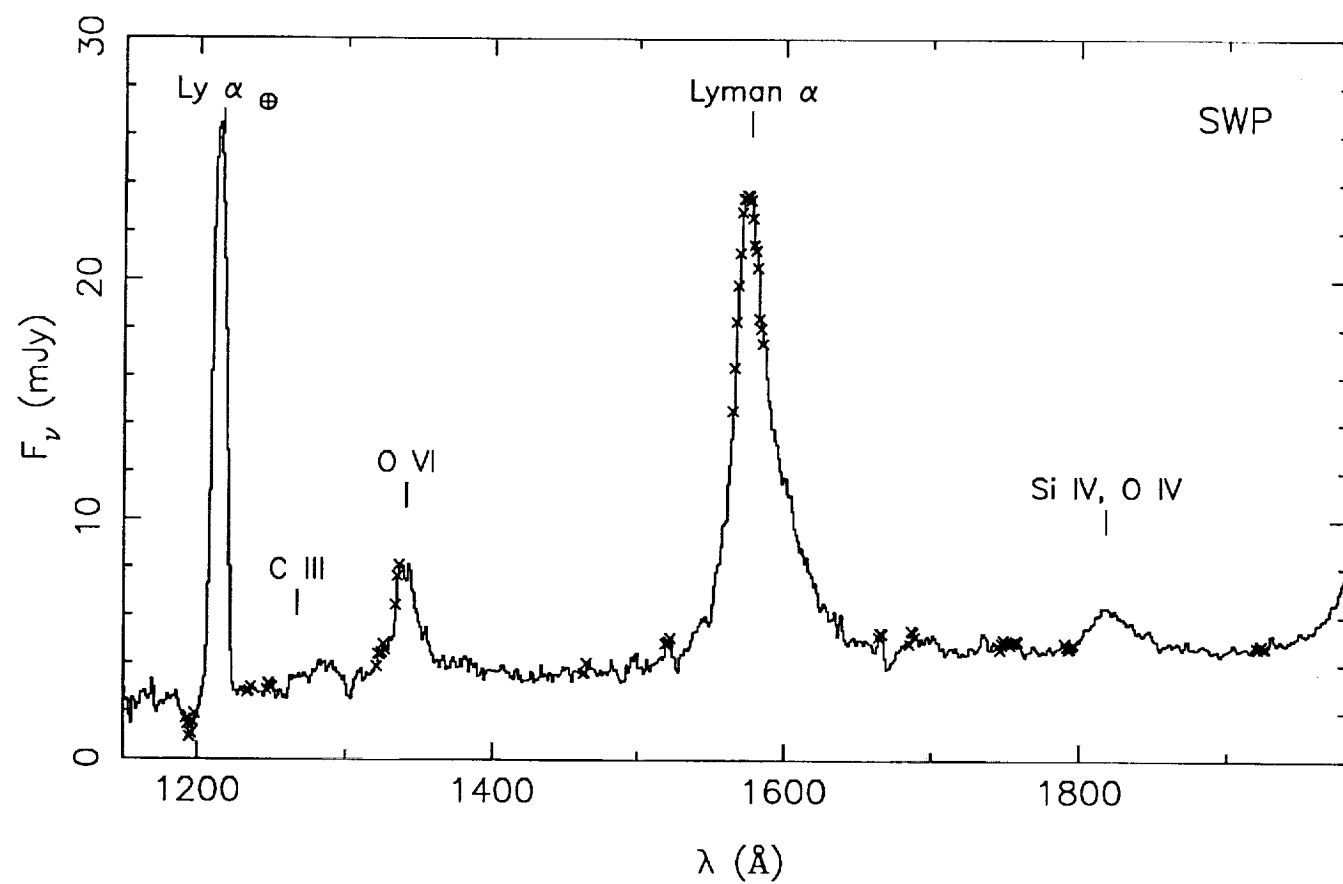


Figure 2

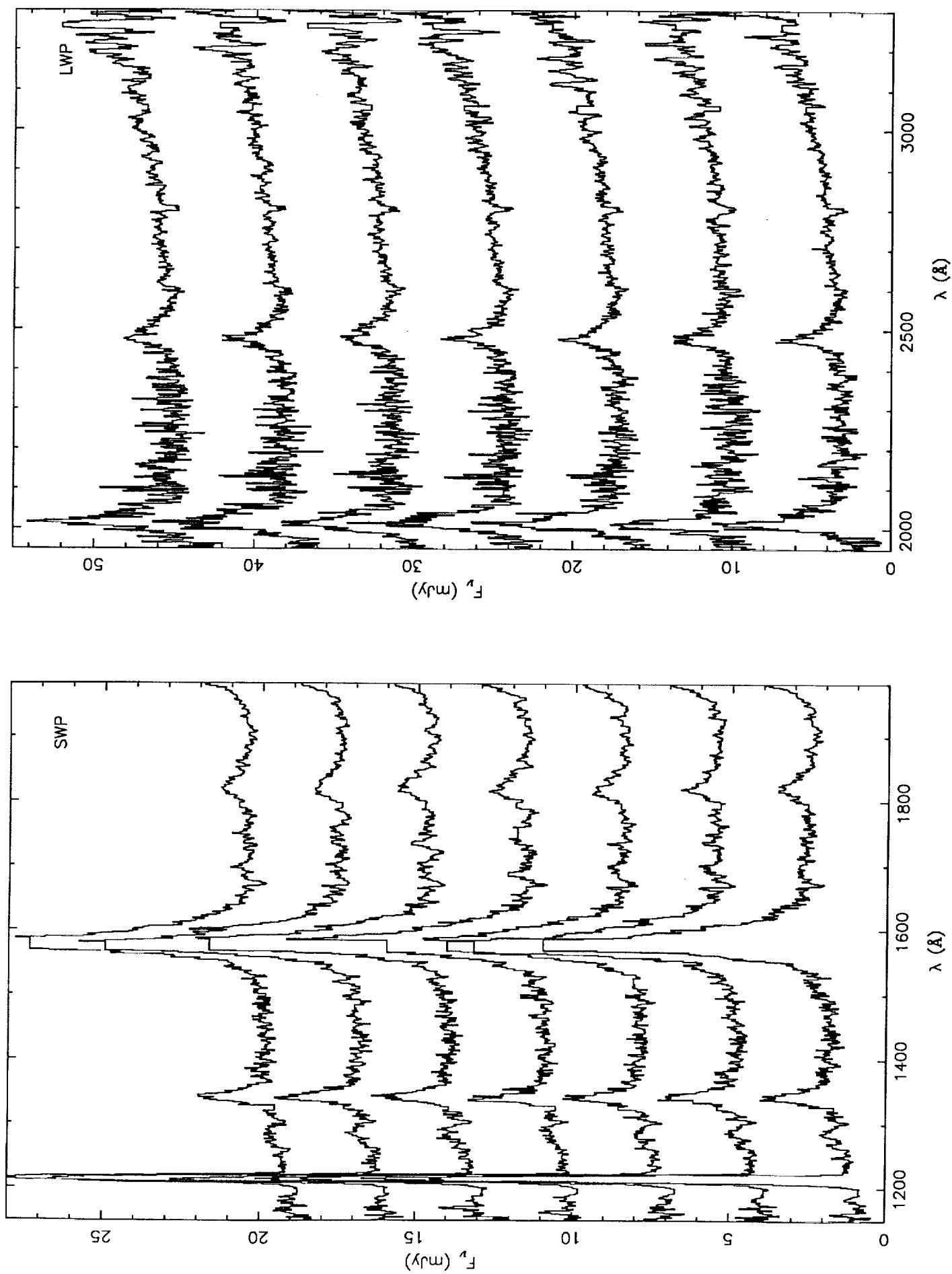


Figure 3

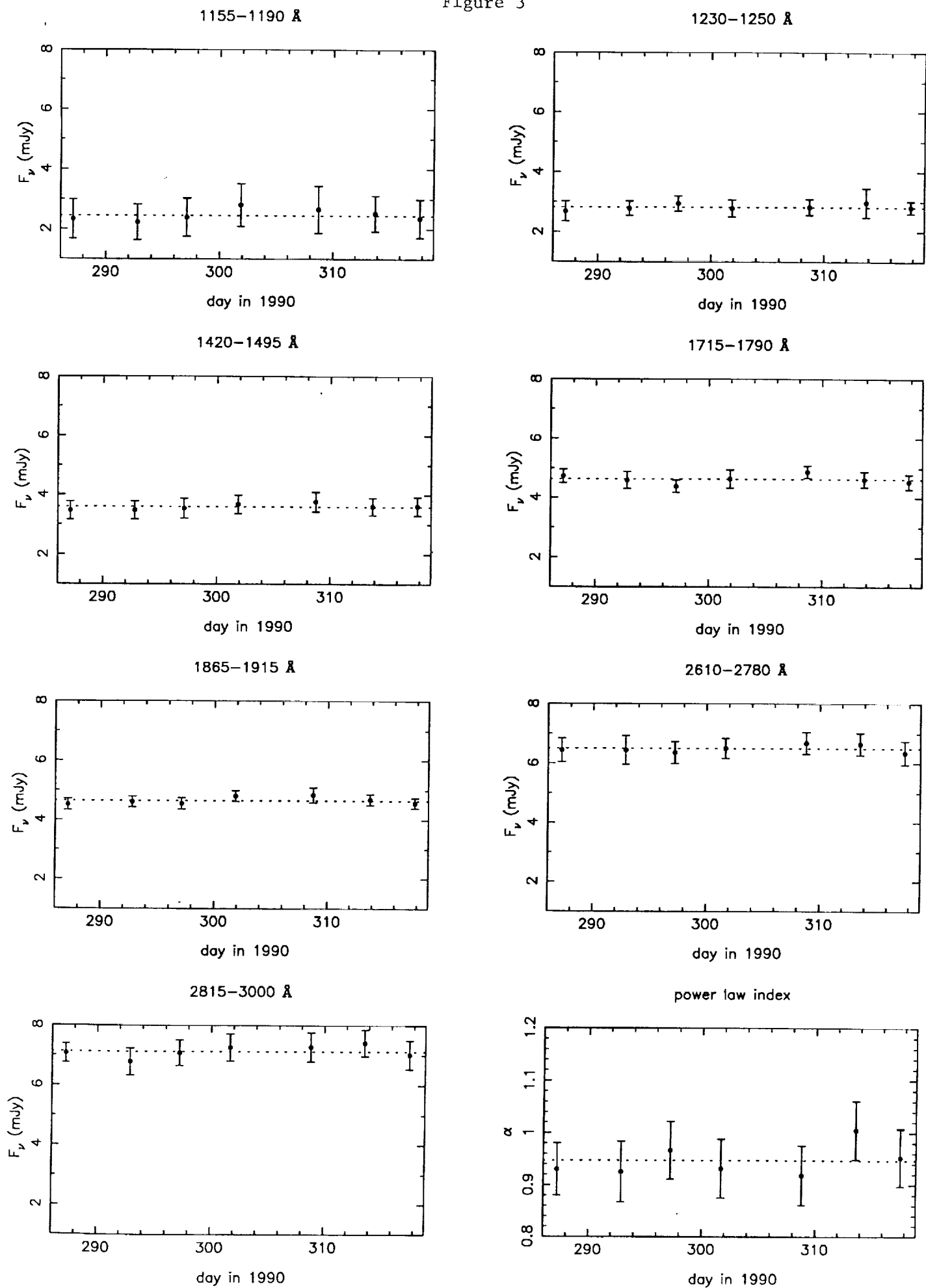
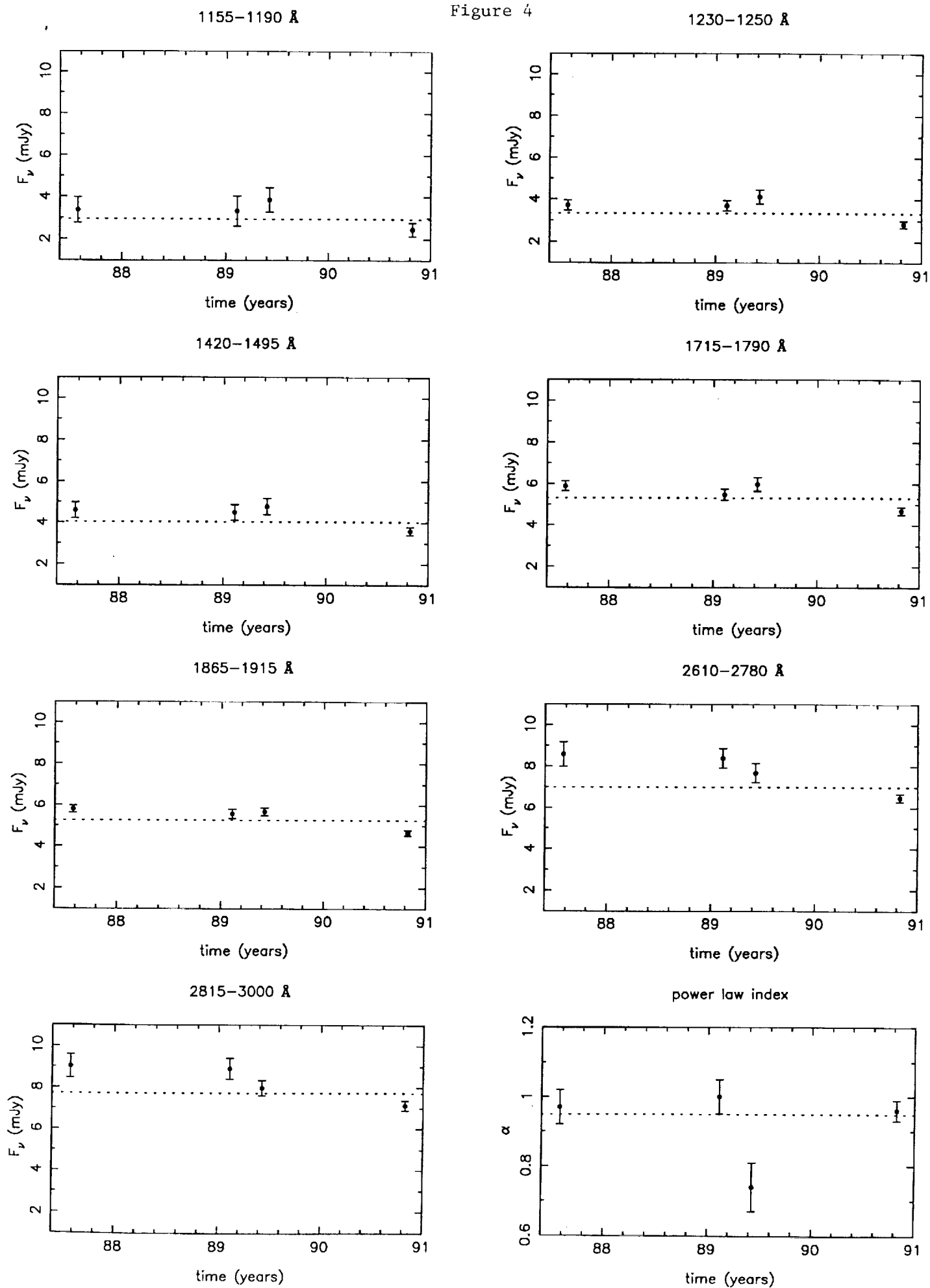


Figure 4



APPENDIX

Papers Published Under NASA Grant NAG 5-1140

“The Ultraviolet Spectrum and Continuum Energy Distribution of the Bright Quasar H1821+643,” M. Kolman, J. P. Halpern, C. R. Shrader, and A. V. Filippenko, *Ap. J.*, **373**, 57 (1991).

“The Redshift of the X-ray Selected BL Lacertae Object H0414+009,” J. P. Halpern, V. S. Chen, G. M. Madejski, and G. A. Chanan, *A. J.*, **101**, 811 (1991).

THE ULTRAVIOLET SPECTRUM AND CONTINUUM ENERGY DISTRIBUTION OF THE BRIGHT QUASAR H1821+643

MICHEL KOLMAN & JULES P. HALPERN¹

Columbia Astrophysics Laboratory, Columbia University, 538 West 120th Street, New York, NY 10027

CHRIS R. SHRADER²

Astronomy Programs, Computer Sciences Corporation

AND

ALEXEI V. FILIPPENKO^{1,3}

Astronomy Department, University of California, Berkeley, CA 94720

Received 1990 August 20; accepted 1990 November 9

ABSTRACT

We report on the first UV observations of the bright QSO H1821+643. With $V = 14.2$ mag and $z = 0.297$, H1821+643 is the second brightest object in the sky at $z > 0.1$. The *IUE* data are combined with new optical spectroscopy, and existing infrared and X-ray data, to reveal a strong optical/UV "big bump," which continues past the Lyman limit in the rest frame of the QSO. A possible turnover at the high-frequency side of the UV continuum constrains fits of a thin accretion disk model to a large black hole mass ($M \simeq 3 \times 10^9 M_\odot$) and high accretion rate ($\dot{M} \simeq 19 M_\odot \text{ yr}^{-1}$), but a small disk size ($R_{\text{out}}/R_{\text{in}} \simeq 12$). The shape of the UV continuum was found to be variable, with a hardening of the spectrum when the source was brighter. Because of its location only 3° from the ecliptic pole, H1821+643 will be an important object for simultaneous UV and soft X-ray monitoring to test for a common origin of the UV bump and soft X-ray excess.

Subject headings: quasars — spectrophotometry — ultraviolet: spectra

1. INTRODUCTION

Twenty years after the discovery of QSOs, one of the brightest objects of this class had yet to be noticed. Known as H1821+643, it was identified by Pravdo & Marshall (1984) as the counterpart of an X-ray source first detected by *HEAO 1* and then by *Einstein*. With $V = 14.2$ mag, it is the brightest object after 3C 273 at $z > 0.1$. The brighter members of a class often contribute disproportionately to our knowledge of their physics, because they can be studied well at many wavelengths. The intermediate redshift of H1821+643 ($z = 0.297$) makes it well-suited to a study of the intrinsic ultraviolet continuum, as higher redshift objects suffer from absorption by intergalactic H I clouds. Moreover, its location only 3° from the ecliptic pole [the position is $\alpha(1950) = 18^{\text{h}}21^{\text{m}}41^{\text{s}}.67$, $\delta(1950) = 64^\circ19'0''.8$] makes H1821+643 an important object for monitoring programs done with satellites. In particular, it is an ideal object to test for a common origin of the UV big bump and the soft X-ray excess, an association which has yet to be proven.

In this paper, we report new ultraviolet and optical spectrophotometry which we combine with existing infrared and X-ray data to study the continuum energy distribution of this QSO. The combined optical and *IUE* spectra show a strong UV bump. The moderate redshift allows the detection of flux past the Lyman limit in the rest frame, while allowing for optimal coverage of the UV bump within the *IUE* bandpass. We present fits to a thin disk model, which require large mass and accretion rate for this high luminosity QSO, but also indicate a small outer radius for the disk.

The strong soft X-ray excess, which was attributed to H1821+643 in the *HEAO A-2* data of 1977, is absent in all

subsequent X-ray observations, which resemble the "canonical" hard power law. Although we take this variable soft excess at face value for the purpose of this paper, we also discuss other soft X-ray sources in the vicinity of the QSO which could have confused the *HEAO A-2* low-energy detector.

2. OBSERVATIONS

2.1. The X-Ray Identification

When H1821+643 was identified by the *Einstein* imaging proportional counter (IPC), comparison with *HEAO A-2* data obtained 3 yr earlier indicated that a factor of 4 decrease in the soft X-ray flux had occurred between 1977 and 1980 (Pravdo & Marshall 1984). The change could be described as the disappearance of the soft X-ray excess, which is clearly present in the *HEAO A-2* low energy detector (LED), and not evident in the *Einstein* IPC. Subsequent observations by *EXOSAT* in 1984 and 1985 (Warwick, Barstow, & Yaqoob 1989) also did not detect a soft X-ray excess, leading these authors to consider the possibility that the *HEAO A-2* LED detector had been confused by another soft X-ray source in the field, possibly the central star of the planetary nebula K1-16 (Grauer & Bond 1984) which is $100''$ from the QSO. But having estimated the flux from K1-16 in the 0.2–2 keV bandpass of the LED, Warwick et al. (1989) concluded that it could not have contributed significantly to the observed soft X-ray excess.

We can further address this issue with the *Einstein* IPC data since the IPC bandpass includes that of the *HEAO A-2* LED. Moreover, the IPC data were taken as part of a survey of the north ecliptic pole region, which can be searched for other soft X-ray sources in the vicinity of the LED error box. There were four overlapping fields, all of which included H1821+643, although in three of these the QSO fell just outside the support ribs of the detector, hampering detailed quantitative analysis.

¹ Guest Observer with the *International Ultraviolet Explorer* Satellite.

² Staff member, *IUE* Observatory, NASA/GSFC. Postal address: Code 668.1, NASA/GSFC, Greenbelt, MD 20771.

³ Presidential Young Investigator.

The X-ray position and pointlike nature of the source in the IPC map are consistent with identification with the QSO and not the planetary nebula, although it cannot be excluded that K1-16 might make a small contribution to the IPC X-ray source. More worrisome for the interpretation of the soft excess in the LED is another X-ray source 36' to the northeast of the QSO, which is of comparable intensity. We identified this source with the 8.0 mag K0 star, SAO 17878. The error boxes of the several *HEAO-1* detectors, in addition to the optical positions of possible confusing sources, are shown in Figure 1. The X-ray flux of SAO 17878 in the 0.1–3.5 keV band as observed with the IPC is 9×10^{-12} ergs cm $^{-2}$ s $^{-1}$, about half that of the QSO at the time of the *Einstein* observations. In the absence of detailed knowledge about its variability, it cannot be ruled out that this star contaminated the LED error box (Nugent et al. 1983), on whose edge it lies. However, the X-ray flux from this star would have to have been at least 4 times larger than the *Einstein* value for it to have made a substantial contribution to the LED flux. The only other X-ray source close to the LED error box is a 5.0 mag F5 star, SAO 17828, with an IPC flux of about 1×10^{-12} ergs cm $^{-2}$ s $^{-1}$. This source is an even less likely contributor. In summary, we can be certain that the hard X-rays arose in the QSO, as indicated by the IPC source and the small *HEAO A-1* error box of 0.05 deg 2 (Wood et al. 1984). We can also be certain that the soft excess was *not* present during the *Einstein* or *EXOSAT* observations. Whether the soft excess observed by the *HEAO A-2* LED arose exclusively in the QSO cannot be determined, although this appears highly likely.

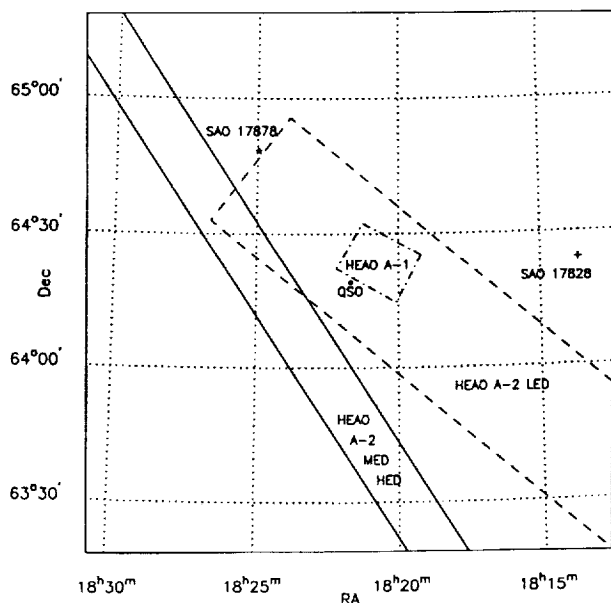


FIG. 1.—Error boxes of the *HEAO* observations around H1821+643 (indicated by the filled circle labeled QSO). The *HEAO A-2* MED-HED error box (Marshall et al. 1979) is indicated by the solid lines; the *HEAO A-2* LED error box (Nugent et al. 1983) is indicated by the dashed lines; the *HEAO A-1* error box (Wood et al. 1984) is indicated by the dot-dashed lines. The star indicates the position of SAO 17878, which could contribute some of the detected flux in the *HEAO A-2* LED band. The plus sign indicates the position of the weak IPC source SAO 17828. The IPC error circles for the QSO and SAO stars have a typical diameter of 1' and are too small to be drawn in this figure. All positions are in 1950 coordinates.

TABLE 1

EINSTEIN IPC SPECTRUM OF H1821+643

Date	1980 May 25
Exposure time (s)	960.0
IPC counts s $^{-1}$ (0.1–3.9 keV)	0.508 ± 0.023
F_x (0.1–3.5 keV) ^a	1.74×10^{-11}
L_x (0.1–3.5 keV) ^b	9.6×10^{45}
A^c	4.23×10^{-3}
α (68% confidence)	0.60 ± 0.34
(90% confidence)	(+0.62, –0.45)
N_H (cm $^{-2}$) (68% confidence)	$2.0 (+1.8, -1.5) \times 10^{20}$
(90% confidence)	$< 5.0 \times 10^{20}$
χ^2_{\min} (per d.o.f.)	1.34

^a Flux (ergs cm $^{-2}$ s $^{-1}$) in observed energy band.

^b Luminosity (ergs s $^{-1}$) in intrinsic energy band, corrected for absorption and assuming $\alpha = 0.6$, $H_0 = 50$ km s $^{-1}$ Mpc $^{-1}$, and $q_0 = 0$.

^c Normalization constant.

2.2. The X-Ray Spectrum

We performed a standard spectral analysis on the single *Einstein* IPC observation in which the QSO fell inside the support ribs. The results are listed in Table 1. Power-law fits yielded a best-fit energy index $\alpha = 0.6$, with 68% confidence limits of 0.26–0.94, and 90% confidence limits of 0.15–1.12. The 90% upper limit on the column density N_H is 5×10^{20} cm $^{-2}$, which is consistent with the 21 cm value of 4.1×10^{20} cm $^{-2}$ (Stark et al. 1990). Hard X-ray spectral measurements by *EXOSAT* (Warwick et al. 1989) and *Ginga* (Turner et al. 1989; Kii et al. 1991) are consistent with an extrapolation of the IPC data, both in spectral index and normalization. Therefore, it seems likely that the soft excess observed by the *HEAO A-2* LED is a separate component, which varies independently of the hard power law.

2.3. The Ultraviolet Observations

In 1987 we obtained the first UV spectra of H1821+643 with the *IUE* satellite. The strong and broad Lyman- α emission line was saturated in the 300 minute exposure of the SWP. A subsequent shorter exposure (120 minutes) resulted in optimal detection in the Lyman- α line. All the *IUE* observations are listed in Table 2. The images were obtained with the large aperture in the low-dispersion mode, resulting in a spectral resolution of about 5 Å and about 8 Å for the SWP and LWP, respectively.

The spectra were obtained from the line-by-line images with the Gaussian extraction routines at the Goddard Regional Data Analysis Facility to minimize the noise while maintaining accurate flux levels. We corrected the spectra for the effects of interstellar reddening, using the extinction curve of Seaton (1979) and $E(B-V) = 0.085$ mag. The color excess is based on

TABLE 2

IUE OBSERVATIONS OF H1821+643

Image	Int. time (minutes)	Date
SWP 31431	300	1987 Jul 29
LWP 11294	130	1987 Jul 29
SWP 31523	120	1987 Aug 10
SWP 35516	275	1989 Feb 9
LWP 14996	95	1989 Feb 9
SWP 36396	300	1989 Jun 4
LWP 15659	120	1989 Jun 4

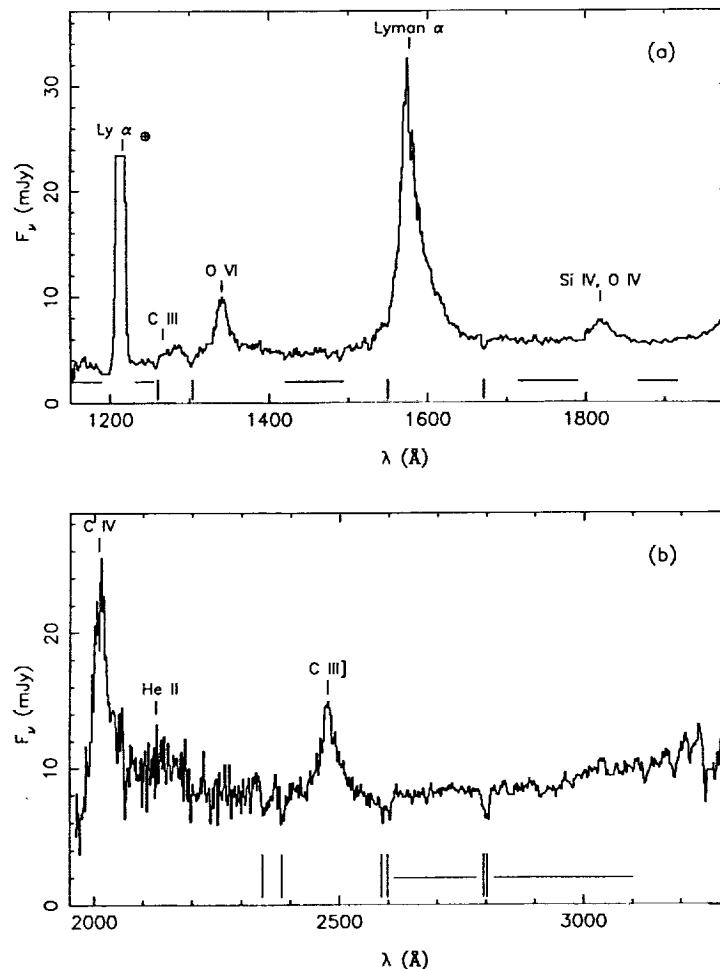


FIG. 2.—(a) Co-added SWP spectrum of H1821+643 obtained with *IUE*, corrected for the estimated interstellar extinction of $E(B-V) = 0.085$ mag. The Lyman- α emission is patched in from the unsaturated image, SWP 31523. (b) LWP spectrum. The horizontal lines denote the wavelengths selected as the continuum and used in Figs. 4 and 6. The vertical tick marks indicate the detected interstellar absorption lines.

the neutral hydrogen column density in the direction of H1821+643 ($N_H = 4.1 \times 10^{20} \text{ cm}^{-2}$, Stark et al. 1990) and the $N_H/E(B-V)$ ratio of $4.8 \times 10^{21} \text{ cm}^{-2} \text{ mag}^{-1}$ (Bohlin, Savage, & Drake 1978). We did not correct for any internal reddening, as there is now growing evidence that the intrinsic extinction in QSOs is very small (Sun & Malkan 1989a, and references therein). We deleted the data points which were flagged because of the presence of a resau. The co-added spectrum is shown in Figure 2. The overall continuum level decreases slightly with increasing frequency. The flux level is sensitive to the correction for interstellar extinction, but even if the spectrum is overcorrected for reddening [up to $E(B-V) = 0.2$ mag], a downward trend with shorter wavelengths remains. Despite the decline in sensitivity below 1200 Å, there is strong emission shortward of the Lyman limit, which is redshifted to 1182 Å (Fig. 3).

As listed in Table 2, there are three series of observations with *IUE*, each resulting in at least one SWP and LWP image: the first in 1987, the second in 1989 February, and the third in 1989 June. Two SWP spectra were obtained in 1987: a long exposure with optimal detection of the continuum level and a short exposure with optimal detection of the Lyman- α emission line. In order to study the continuum, the spectra were binned into about 10 data points per camera, avoiding the

major emission lines and the Galactic absorption lines. If we compare these three series of observations, no significant changes could be found between the first and second series, while the spectral shape did change significantly between the second and third series. As shown in Figure 4, the emission between 2000 and 3000 Å decreased in intensity, while the short wavelength side increased by about 10%, resulting in a hardening of the spectrum between 1989 February and June.

2.4. Optical Spectroscopy

Optical CCD spectra of H1821+643 covering the wavelength range 3138–10046 Å were obtained on 1988 October 3 UT using four different grating settings of the UV Schmidt spectrograph (Miller & Stone 1987) at the Cassegrain focus of the Shane 3 m reflector at Lick Observatory. The spectra were obtained through a long slit of width 8", oriented along the parallactic angle (Filippenko 1982). The airmass was 1.3, conditions were photometric, and the seeing was about 1". Typical integration times per setting were 300–500 s. The spectral resolution was 5–8 Å below about 7200 Å, and 10–16 Å in the near-IR region.

Standard techniques were used to extract one-dimensional spectra from the CCD data. These included subtraction of the bias level, division by a flat field, removal of cosmic rays, cor-

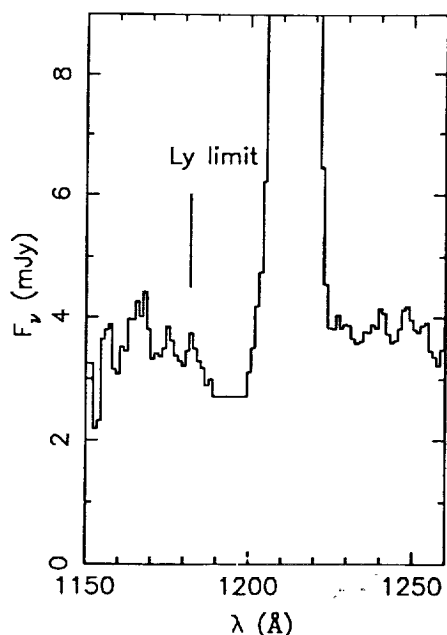


FIG. 3.—Expanded view of Fig. 2a shows the presence of substantial flux below the Lyman limit at 1182 Å (indicated by the vertical tick-mark). We estimate that the covering fraction at the Lyman limit must be less than 0.09. The strong emission line around 1216 Å is geocoronal Lyman- α . The data points around 1190 Å are deleted because of the presence of reseau.

rection for geometric distortion and misalignments, and subtraction of the background sky. Several stars from the lists of Oke & Gunn (1983) and Massey et al. (1988) were used to flux calibrate the spectra, as well as to remove telluric absorption bands at wavelengths longer than 6200 Å. Excellent agreement in absolute fluxes and spectral shapes was found in overlapping spectral regions. However, the wavelength scale is uncertain by about 4 Å, since the observations were obtained through a wide slit. The redshift derived from the [O III] lines is 0.2972 ± 0.0006 .

The overall optical spectrum of H1821+643, corrected for extinction [$E(B-V) = 0.085$ mag], is shown in Figure 5. The near-UV flux joins that of the *IUE* spectrum very well, as can be seen by comparison of Figures 2 and 5.

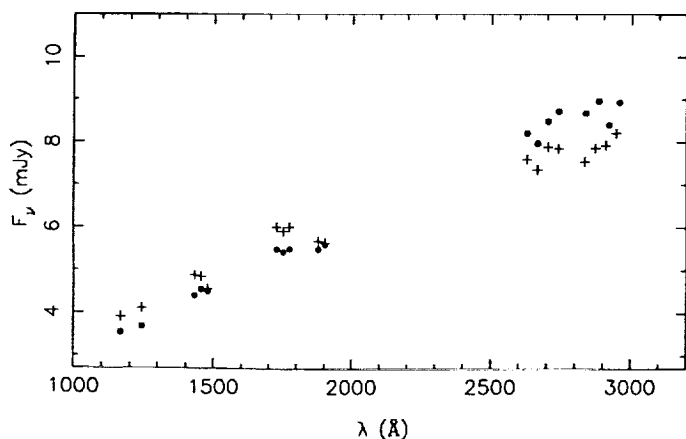


FIG. 4.—Change in the UV continuum shape between 1989 February 9 (indicated by filled circles) and 1989 June 4 (indicated by plus signs). The flux increased by about 10% at the shortest wavelengths while the flux decreased at the long-wavelength side, corresponding to a hardening of the spectrum.

2.5. Optical and Infrared Photometry

The *UBV* photometry was obtained by S. Vrtilek with the 0.9 m telescope at Kitt Peak National Observatory on 5 nights centered around 1988 October 10. Variability in the *V* band was less than 0.03 mag from night to night, and less than 0.04 mag and 0.2 mag for *B-V* and *U-B*, respectively. The average magnitudes are listed in Table 3. Near infrared magnitudes from the Infrared Telescope Facility (IRTF) in the *J* (1.25 μ m), *H* (1.65 μ m), *K* (2.2 μ m), and *L'* (3.8 μ m) bands were provided by M. Elvis, and are listed in Table 3. In the far infrared, *IRAS* detections in all four bands were published by Neugebauer et al. (1986), and are also listed in Table 3.

The overall continuum distribution derived from all the above data and shifted to the rest-frame is shown in Figure 6. Throughout this article λ and ν denote observed wavelength and frequency, while λ_0 and ν_0 denote the wavelength and frequency in the rest-frame of the QSO.

2.6. Radio Observations

VLA observations at 6 cm with a partial array of six dishes and an exposure time of 20 minutes yielded an upper limit of 15 mJy, establishing this QSO as radio quiet.

3. RESULTS

3.1. Emission Shortward of the Lyman limit

The redshift of H1821+643 (0.297) is high enough to shift the Lyman limit to 1182 Å, into the wavelength range of *IUE*, but low enough to avoid absorption by intervening H I clouds. Substantial flux is detected below 1182 Å in all our SWP spectra (Fig. 2). An upper limit to the covered fraction of the continuum source as derived from the flux levels below and above 1182 Å is estimated at 0.09; a small value consistent with the absence of X-ray absorption in this and other bright AGNs. This small covering fraction of less than 0.1 is also expected in a high luminosity QSO such as H1821+643 on the basis of photon counting arguments concerning the photoionization of clouds on the BLR. Rest-frame Lyman continuum absorption has been reported (Kinney et al. 1985) in less than 10% of all AGNs. Another bright QSO, 3C273, is a possible

TABLE 3
PHOTOMETRY OF H1821+643

Band	Magnitude	Flux (mJy)
U ^a	13.30	9.04
B ^a	14.30	8.12
V ^a	14.26	7.55
J ^b	13.09	8.8
H ^b	12.19	13.0
K ^b	11.12	22.1
L ^b	8.95	60.5
12 μ m ^c		236
25 μ m ^c		373
60 μ m ^c		953
100 μ m ^c		2164
6 cm		<15

^a Magnitude averaged over 5 nights, obtained with the automated filter photometer on the 0.9 m telescope at Kitt Peak National Observatory around 1988 October 10 (S. Vrtilek 1988, private communication).

^b IRTF instrumental magnitude, obtained with 6" diameter aperture and the InSb detector (RC2) on 1988 April 25 (M. Elvis 1988, private communication).

^c *IRAS* fluxes (Neugebauer et al. 1986).

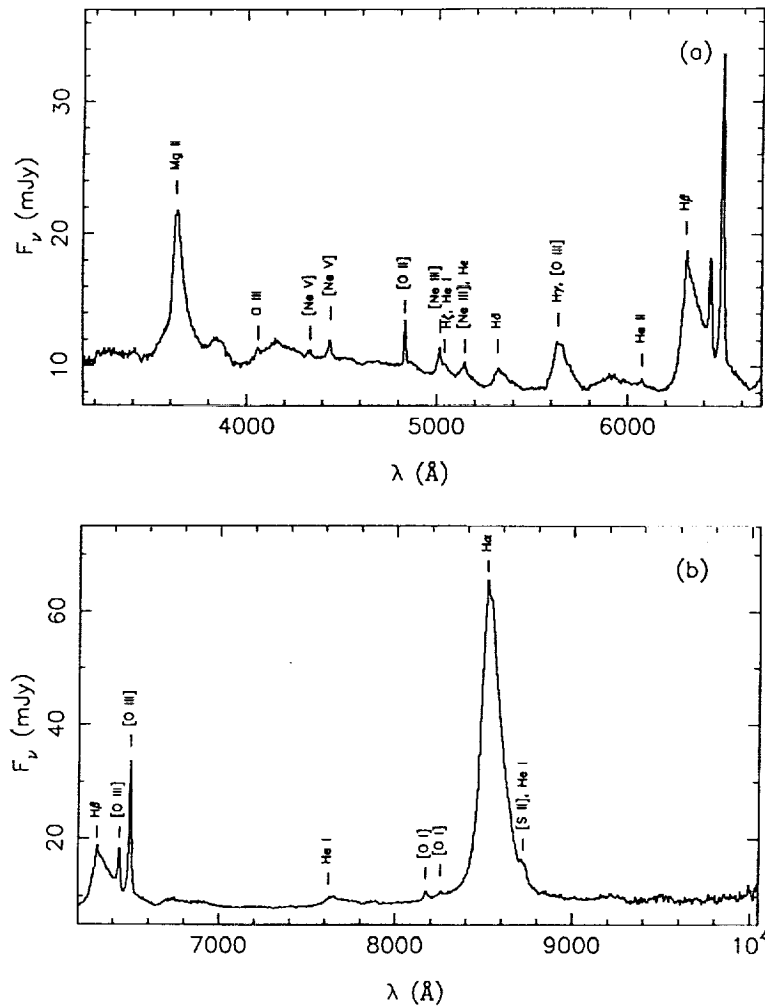


FIG. 5.—Optical spectrum of H1821+643 obtained at Lick Observatory on 1988 October 3 under photometric conditions. The interstellar extinction correction for $E(B-V) = 0.085$ mag has been applied. The continuum appears bumpy due to the contribution of blended Fe II lines (e.g., around 3800, 4200, 5900, and 6700 Å).

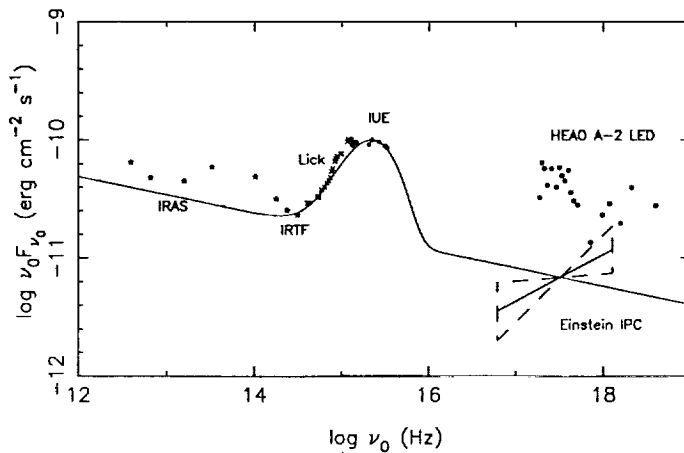


FIG. 6.—Overall continuum spectrum of H1821+643 plotted in the QSO rest frame, with the co-added *IUE* data from 1987. Note the turnover of the UV bump and the large amplitude variation between the X-ray observations. The power-law plus thin accretion disk (solid line) fit with $M = 3 \times 10^9 M_\odot$, $\dot{M} = 19 M_\odot \text{ yr}^{-1}$, and $R_{\text{out}}/R_{\text{in}} = 12$, deviates between $\log \nu_0 = 14.8$ and $\log \nu_0 = 15.2$ due to the Balmer continuum and Fe II line emission.

exception, as a Lyman discontinuity has been reported in combined *IUE/Voyager* data (Reichert et al. 1988). By contrast, the continuum spectrum of H1821+643 seems to turn over smoothly well longward of the Lyman limit, which argues that the thermal peak, rather than any Lyman limit absorption, is responsible for the drop in flux level at the high-frequency side of the *IUE* spectrum. However, one must be aware of the possibility that Lyman continuum absorption is an intrinsic property of accretion disks in AGNs (Sun & Malkan 1987; Sun & Malkan 1989b; Scott & O'Dell 1989), and that a suitable smearing of the Lyman edge due to strong Doppler and gravitational effects in the inner disk might cause some of the turn-over which is observed.

3.2. Continuum Energy Distribution

None of the observations in different wavebands were simultaneous; nevertheless, the infrared through UV data are very continuous. There is a steep rise in the flux level at optical frequencies, and the *IUE* data points indicate a strong UV bump. The prominence of the UV bump is similar to the one detected in the optical/UV bump prototype PG 1211+143, but it could be observed to higher rest-frame frequencies due to the higher redshift ($z = 0.297$ vs. $z = 0.085$ for PG 1211+143).

In all the spectra except the one obtained in 1989 June, there is evidence for a turnover at the high-frequency side (around $\log \nu_0 = 15.3$).

Because of the 5 μm feature displayed by the IR data points, the power law, if any, is not well defined in the infrared. By forcing a fit to the 60 μm and 1 μm data points, we find $\alpha = 1.16$ (where $F_\nu \propto \nu^{-\alpha}$). Because there is a strong correlation between the IR and hard X-rays in QSOs (Edelson & Malkan 1986; Kriss 1988), a single power law might be extrapolated from $\log \nu_0 \approx 12$ to $\log \nu_0 \approx 18$. The turn-up from the overall power law of the hard X-ray data (both for the *Einstein* data and the 2–10 keV *HEAO 1* data) is typical for the high-frequency side of the continuum energy distribution in QSOs (Elvis 1988). Considering the large amplitude of variability in the X-rays, it is impossible to estimate the soft X-ray flux level at the time of the *IUE* observations, which would be important for models of the soft X-ray excess.

3.3. Emission Lines

Information on continuum emission in the unobservable EUV gap can be derived from the UV and optical emission lines, which are powered by photons with EUV energies. To this end, we measured the major emission lines in the UV and optical spectra. No significant differences in line fluxes were found from one *IUE* observation to the other; therefore, all the *IUE* spectra were coadded and dereddened. The measured line properties are listed in Table 4 and the lines are identified in Figures 2 and 5. The Lyman- α emission line could only be

TABLE 4
EMISSION-LINE MEASUREMENTS OF H1821 + 643

ID ^a	Intensity ^b	Flux ^c	EW ^d (Å)
C III $\lambda 2777$	< 35.0	< 20.3	< 5.0
O VI $\lambda 1034^e$	137.1	83.4	16.8
Ly α $\lambda 1216$, (N V $\lambda 1240$)	963.5	626.9	156.0
Si IV $\lambda 1397$, O IV $\lambda 1407$	49.8	32.8	10.0
C IV $\lambda 1549$	504.8	305.9	111.4
He II $\lambda 1640$, (O III] $\lambda 1663$)	161.9	91.7	36.8
C III] $\lambda 1909$	115.2	78.1	30.4
Mg II $\lambda 2798$	222.6	186.5	98.7
O III $\lambda 3133$	1.8	1.6	1.0
[Ne V] $\lambda 3345$	2.1	1.8	1.3
[Ne V] $\lambda 3426$	4.3	3.8	2.8
[O II] $\lambda 3727$	5.1	4.6	4.1
[Ne III] $\lambda 3869$	4.5	4.2	4.7
H ζ $\lambda 3889$, He I $\lambda 3888$	2.4	2.2	2.5
[Ne III] $\lambda 3968$, He I $\lambda 3970$	3.6	3.3	3.6
H δ $\lambda 4102$	11.0	10.3	13.2
H γ $\lambda 4340$, [O III] $\lambda 4363$	29.0	27.8	39.3
He II $\lambda 4686$	0.6	0.6	1.0
H β $\lambda 4861$	100.0	100.0	172.6
[O III] $\lambda 4959$	8.4	8.3	10.4
[O III] $\lambda 5007$	28.6	28.4	40.3
He I $\lambda 5876$	9.8	10.2	24.0
[O I] $\lambda 6300$	1.6	1.7	4.0
[O I] $\lambda 6363$, ([Fe x] $\lambda 6375$)	0.9	0.9	2.0
H α $\lambda 6563$, ([N II] $\lambda 6548, 83$)	333.3	352.3	895.1
[S II] $\lambda 6716, 30$ (He I $\lambda 6678$)	4.8	5.1	9.9

^a Identification of emission line and rest wavelength; the lines in parentheses denote only minor contributions.

^b Intensity corrected for Galactic reddening, relative to H β , with $I(\text{H}\beta) = 1.05 \times 10^{-12} \text{ ergs cm}^{-2} \text{ s}^{-1}$.

^c Observed flux relative to H β with $F(\text{H}\beta) = 8.63 \times 10^{-13} \text{ ergs cm}^{-2} \text{ s}^{-1}$.

^d Observed equivalent width.

^e Narrow component only (FWOI ~ 40 Å).

measured in SWP 31523, as the other SWP spectra were saturated at this line. The major source of error in the line measurements is the uncertainty in the continuum level, which is contaminated by the broad wings of the emission lines, Galactic absorption lines, and blended Fe II line and Balmer continuum emission. For the O VI $\lambda 1034$ emission line only the narrow component was measured (with a full width at zero intensity, FWOI, of about 40 Å), as it was unclear to where the broad wings extend (possibly from 1280 to 1380 Å, encompassing the Galactic absorption feature around 1300 Å). This uncertainty around the O VI line also complicated the measurement of the upper limit to C III $\lambda 2777$ at its redshifted wavelength of 1267 Å, as well as the measurement of the O I $\lambda 1302$, Si II $\lambda 1304$ absorption feature.

These UV observations are the first to be conducted for H1821 + 643. There were, however, previous optical observations with emission line measurements from 1981 (Pravdo & Marshall 1984). The equivalent widths listed by these authors for Mg II, H γ and H β are smaller (by about 30%) than our measurements, and larger (by 15%) for [O III] $\lambda 5007$. Compared to a sample of 20 intermediate redshift QSOs ($z < 0.84$, Kinney et al. 1985) the EW of Lyman- α for H1821 + 643 is typical, being close to the sample's average. Kwan & Krolik (1981) compiled the average and range of permitted line ratios for a large sample of QSOs. No single line ratio observed in H1821 + 643 is outside this sample's range. Compared to the mean, the observed ratios of Ly α /H β , C IV $\lambda 1549$ /Ly α , and Mg II $\lambda 2798$ /H β in H1821 + 643 are large (by a factor of about 1.5), while the C III] $\lambda 1909$ /C IV $\lambda 1549$ ratio is half the mean value.

Considering the overall energy distribution of H1821 + 643, it would be of interest to determine where the spectrum peaks: at *IUE* frequencies as suggested by the detected turnover, at soft X-ray energies as indicated by the *HEAO 1* data, or in the unobservable EUV gap. Krolik & Kallman (1988) investigated this question theoretically by modeling the effects of the several different accretion disk spectra [i.e., bare power law, power law plus disk spectrum peaking at 10 eV ($\log \nu_0 \sim 15.4$), and one peaking at 80 eV ($\log \nu_0 \sim 16.3$)] on the emission line formation. Although the ionization parameter Ξ is far more important than the shape of the ionizing spectrum in determining the line emission, there are line ratios which are relatively insensitive to the ionization parameter.

The observed line ratios in H1821 + 643 are consistent with a power law plus disk spectrum peaking at 10 eV, i.e., in the UV, within the context of the Krolik & Kallman (1988) model. All ratios are within the model range (with the pressure as a free parameter between 6.3×10^{13} and $20 \times 10^{13} \text{ K cm}^{-3}$) for the high ionization case ($\Xi = 2.0$), except for C III] $\lambda 1909$ /C IV $\lambda 1549$ (the one ratio that is substantially smaller than the average value for Kwan & Krolik's 1981 sample of AGNs). A high Ξ might be expected for an ionizing spectrum peaking at low energies in order to produce enough high-ionization species.

3.4. Absorption Lines

The location of H1821 + 643 at (l, b) = ($94^\circ, 27^\circ$) and the moderate column density of $4.1 \times 10^{20} \text{ cm}^{-2}$ are ideal for study of interstellar absorption. The Galactic longitude of H1821 + 643 permits optimal velocity separation of distant matter from local matter, while the low-latitude permits the viewing of distant matter at large height above the Galactic plane. Therefore, future high-resolution studies of the absorp-

TABLE 5
ABSORPTION-LINE MEASUREMENTS OF H1821+643

ID	EW (Å)
S II λ 1251, 1254, 1260, Si II λ 1260	0.8
O I λ 1302, Si II λ 1304	2.6
C IV λ 1548, 51	<0.7
Al II λ 1671	0.6
Fe II λ 2343	2.8
Fe II λ 2374, 2382	3.5
Fe II λ 2586	1.6
Fe II λ 2599	1.8
Mg II λ 2796, 2803	3.9

tion features in H1821+643 could investigate the properties of the interstellar medium at large galactocentric distances. We measured the absorption lines listed in Table 5 and indicated by tick marks in Figure 2. The lines are from low-ionization species, except for C IV for which only an upper limit is obtained due to its location on the blue wing of Lyman- α . The C IV λ 1548, 1551 absorption is thought to arise in the Galactic halo (Savage 1988). We did not detect any absorption lines in the optical spectrum. An extensive compilation of EWs of absorption lines arising at higher Galactic latitude ($b \sim 60^\circ$, Savage 1988) gives lower values than ours (typically by a factor of about 2) for the low-ionization species except S II, Si II and Al II. Other studies of absorption features arising at lower latitudes [(l, b) = ($96^\circ, 12^\circ$), Pettini et al. 1982] show the same strong absorption in Mg II λ 2796, 2803 and Fe II λ 2599 as we measured in H1821+643.

In H1821+643, the spectral region between Lyman- α and C IV λ 1549 covers the redshift range 0.04–0.27 for detection of C IV absorption lines arising between the QSO and our Galaxy. In this sensitive part of the SWP camera no such absorption features were found above the detection threshold of EW ~ 0.3 Å. The spectral region shortward of the Lyman α emission line allows the detection of low-redshift Lyman α forest lines. Although in the co-added SWP spectrum there are several possible absorption features in this region (e.g., at $\lambda \sim 1470$ and 1490 Å), none were present persistently in all four SWP spectra. The absence of intergalactic Lyman- α and C IV lines is expected for the low redshift of H1821+643 (Bergeron 1988).

4. ACCRETION DISK MODELS

Through studies of variability at different wavelengths (Cutri et al. 1985), and continuum energy distributions between IR, optical, UV, and X-rays (Malkan & Sargent 1982), it has been established that the optical/UV bump is a separate feature from the underlying power law and is now usually attributed to an accretion disk.

In the original model of Shakura & Sunyaev (1973), a summation of Planckian emission arises from the geometrically thin (but optically thick) accretion disk. At the high-frequency side a turnover occurs, corresponding to that blackbody curve with the maximal temperature at the inner disk. There are two free parameters in this model (in addition to the inclination i , and the outer radius of the disk, which affects the low-energy side): the mass M of the central black hole and the accretion rate \dot{M} . In addition, the optical continuum generally deviates from the overall power law around 3000 Å. This emission is attributed to Balmer continuum and blended Fe II line emission (Wills, Netzer, & Wills 1985).

Several modifications to the original model have been suggested: inclusion of opacity (e.g., electron scattering and Comptonization) and inclination effects (Czerny & Elvis 1987; Wandel & Petrosian 1988). The Comptonization hardens the emitted spectrum without increasing the energy requirements, and therefore keeps the luminosity sub-Eddington. One of the inclination effects is relativistic focussing of the innermost rays along the disk (Cunningham 1975), resulting in harder spectra for disks which are viewed edge-on. The effects of scattering around the disk have been modeled using stellar atmospheres (Sun & Malkan 1987), resulting in a strong Lyman limit absorption edge for disks observed face-on. However, these authors indicate that blackbody disk models fit the observations better than the models using stellar atmospheres (Sun & Malkan 1989a).

Although alternatives to the thin accretion disk models are available (e.g., the thick torus model by Madau 1988), thin disks are widely used as these have been shown to fit observations of QSOs and Seyfert 1 galaxies successfully (Malkan & Sargent 1982). We calculated disk models for a nonrotating black hole ($a/M = 0$, the Newtonian case), with the standard assumption that the emerging radiation can be described locally by a blackbody spectrum. The temperature T at radius R is given by

$$T(R) = \left\{ \frac{3GM\dot{M}}{8\pi\sigma R^3} \left[1 - \left(\frac{R_{in}}{R} \right)^{1/2} \right] \right\}^{1/4}, \quad (1)$$

where R_{in} is the innermost stable orbit ($R_{in} = 3R_{Sch}$, Shakura & Sunyaev 1973). We did not include relativistic effects, since the disk around a nonrotating black hole does not reach close to the black hole (unlike the case of the rotating black hole, where the disk reaches much closer) and the relativistic contributions are, therefore, relatively small. The emergent flux is calculated after fixing the inclination angle such that $\cos i = 0.5$ and assuming a distance D given by

$$D = \frac{cz}{H_0} \left(1 + \frac{z}{2} \right), \quad (2)$$

for $q_0 = 0$ and $H_0 = 50 \text{ km s}^{-1} \text{ Mpc}^{-1}$. We did not include a fitting component to account for the Balmer continuum and blended Fe II line emission, and, therefore, our fits deviate from the observed data points between $\log v_0 \sim 14.8$ and $\log v_0 \sim 15.2$.

The best-fit (by eye) to the 1987 IUE data, as shown in Figure 6, with a thin accretion disk model added to the power law, is satisfactory to explain the optical/UV spectrum with the following fitting parameters: $M = (3 \pm 0.5) \times 10^9 M_\odot$, $\dot{M} = 19 \pm 3 M_\odot \text{ yr}^{-1}$, $R_{out}/R_{in} = 12(+5, -3)$, ($L/L_{Edd} = 0.16$). The fit is constrained at both the high-energy side because of the turnover of the high-frequency IUE data points and at the low-energy side due to the steep rise of optical data points. The major sources of uncertainty in the fitting parameters are (1) the nonsimultaneity of the optical and UV data points, (2) the contribution of the Balmer continuum and the Fe II lines, and (3) the correction for interstellar reddening. In this model, the mass of the central object determines mainly the frequency of the peak, while the accretion rate determines mostly the normalization. Once these two parameters have been determined by the turnover in the UV and the strength of the optical/UV bump, respectively, the width of the bump is determined by the extent of the disk, i.e., the ratio R_{out}/R_{in} . The lower limit to R_{out}/R_{in} rules out the possibility of a single blackbody fit, which

would result in a far too narrow bump. If the reality of the UV turnover seen around $\log \nu_0 = 15.3$ is doubted, then the bump could peak at higher frequencies, outside the range of *IUE*. In that case, M would be smaller and the bump would be wider requiring a larger disk (possibly increasing $R_{\text{out}}/R_{\text{in}}$ to about 30). Such a result is within the range of acceptable fits to the 1989 June *IUE* data, as the short-wavelength turnover is not apparent then. To estimate the uncertainty due to the interstellar reddening correction, we found that $E(B-V) = 0.1$ mag (an increase by about 20%), would increase \dot{M} by about 10%, while M and the size of the disk would remain unchanged. The use of a color excess of $E(B-V) = 0.12$ mag or higher would result in a dereddened spectrum without a turnover, again increasing the uncertainty in M and $R_{\text{out}}/R_{\text{in}}$. However, such a large color excess would correspond to a hydrogen column density of $5.8 \times 10^{20} \text{ cm}^{-2}$, far above the values measured near H1821+643.

The novel result of this analysis is the relatively small value of $R_{\text{out}}/R_{\text{in}}$ (9–17). Bechtold et al. (1987) applied a similar fitting model to the spectrum of PG 1211+143 and found a best fit $R_{\text{out}}/R_{\text{in}}$ of at least 200, considerably larger than we found in H1821+643. It is of interest to note that the unexpectedly small outer radius in H1821+643 could be identified with the maximum or critical radius (R_{crit}) in the so-called two-temperature accretion flow model of Begelman, Sikora, & Rees (1987). These authors studied the ion torus around a central black hole, and in particular, the cooling effects of electron-positron pair production on such a torus. Due to these cooling effects the torus collapses to a geometrically thin, optically thick annulus in the innermost region, defined by $R < R_{\text{crit}} \sim 30 R_{\text{Sch}}$. The thermal UV and possibly the soft X-rays would come from this optically thick region, which would in fact have an outer radius remarkably close to our fit value $R_{\text{out}} = 36 R_{\text{Sch}}$ ($R_{\text{out}}/R_{\text{in}} = 12$). In this model, due to the bistability of the annulus, smooth changes in \dot{M} would cause abrupt changes in the flow structure, which in turn would be responsible for spectral variations. In a stable disk, changes in \dot{M} would affect the emergent spectrum only on the viscosity time scale t_{vis} (Bechtold et al. 1987); for an α disk with the parameters inferred for H1821+643 above, t_{vis} is greater than 6000 yr for $\alpha < 1.0$ (Frank, King, & Raine 1985).

A successful fit of both the optical/UV bump and the *HEAO 1* soft X-ray excess is practically impossible to achieve, considering the decline of the *IUE* data points, and the high and fairly constant flux level for the 0.5–2 keV *HEAO 1* observations. If such a fit is forced (ignoring the nonsimultaneity of the UV and X-ray data), highly super-Eddington luminosities ($L \sim 40 L_{\text{edd}}$) would be produced for the Newtonian accretion disk models, violating the thin disk approximation for the inner disk (Bechtold et al. 1987), unless Compton scattering of the UV photons to EUV and soft X-ray energies is incorporated (Czerny & Elvis 1987). While following the optical data points rather closely, such a fit exceeds the observed UV flux by a factor of about 2–3. Moreover, as there is no evidence that the UV emission and the soft X-ray excess are linked in AGNs (Elvis, Wilkes, & McDowell 1989), there is no convincing justification to fit both features in one model fit for H1821+643 at this moment. This QSO would, however, be an excellent candidate to study whether the UV and soft X-ray radiation have the same physical origin, considering the variability and brightness of both the UV and X-ray emission. In Figure 4 the change in the UV continuum over a period of 4 months is shown. This change in shape, where the spectral hardness is

correlated with luminosity, is often found in AGNs which are well observed with *IUE* (Edelson, Krolik, & Pike 1990) and is consistent with an expected increase of temperature with accretion rate. The reported minimum doubling time of about 10 days at X-ray energies (Snyder & Wood 1984) could be identified with the dynamical time scale (t_{dyn}) of the inner disk. We define t_{dyn} as $(1+z) R_{\text{max}}/v_{\text{max}}$, where R_{max} is the radius at which the temperature of the disk reaches a maximum ($R_{\text{max}} \sim 8GM/c^2$) and $v_{\text{max}} = (GM/R_{\text{max}})^{1/2}$. Thus, $t_{\text{dyn}} = GM/(8c^2)^{3/2} (1+z)$ as seen by the observer, or $t_{\text{dyn}} \sim 1.7 (M/10^9 M_{\odot})$ days.

Sun & Malkan (1989a) presented fits of a thin accretion disk model to the spectra of 24 AGNs, not including H1821+643. As the inferred disk parameters are very similar in the Schwarzschild metric (used by Sun & Malkan 1989a) and the Newtonian metric (used here) for $\cos i = 0.5$, we can compare our values obtained for mass and accretion rate with the large sample. With $M = 3 \times 10^9 M_{\odot}$, H1821+643 would be one of the most massive AGNs in the sample and the most massive of the AGNs with intermediate redshift ($z = 0.2$ – 1.0). The inferred accretion rate of $\dot{M} = 19 M_{\odot} \text{ yr}^{-1}$ would be one of the highest for an intermediate redshift QSOs. This was to be expected, considering the large luminosity of H1821+643 and the pronounced optical/UV bump in its spectrum.

There is, however, one significant difference between our model and that of Sun & Malkan (1989a), and that is the use of the outer radius of the accretion disk. Sun & Malkan (1989a) do not specify their outer radius, but it can be assumed to be a large value. In our fitting model the outer radius is a free parameter, resulting typically in low inferred values for successful fits ($R_{\text{out}}/R_{\text{in}} \sim 12$). A strong UV/optical bump with a small width, as is the case for H1821+643, can only be fitted in a satisfactory manner with a small accretion disk. While the turnover and the height of the UV bump determine the central mass and accretion rate, the extent of the disk is determined by the width of the bump. We maintain that only a limited disk, in which the range of temperatures is small and therefore the emergent spectrum only slightly broader than the single black-body curve, fits a narrow optical/UV bump, as observed in H1821+643.

5. CONCLUSIONS

We have obtained multiwavelength observations of H1821+643 and have modeled its continuum with an accretion disk in addition to an underlying power law. The continuum follows the power law with $\alpha = 1.16$ most closely in the far-IR and near-IR, deviating strongly at optical and UV frequencies, and possibly at soft X-ray energies. Most of the energy is emitted in the UV, while the variable soft X-ray excess could have a similar luminosity when at maximum. Fits with a geometrically thin, optically thick accretion disk yield a central black hole mass of $3 \times 10^9 M_{\odot}$ and an accretion rate of $19 M_{\odot} \text{ yr}^{-1}$, both large values consistent with the luminosity of H1821+643 and the prominence of the optical/UV bump in its continuum spectrum. The accretion disk fits result in a surprisingly small disk size ($R_{\text{out}}/R_{\text{in}} = 12$). Efforts to constrain the extreme UV spectrum by applying photoionization models, which predict emission line ratios, were indicative of an ionizing spectrum peaking at UV frequencies.

The shape of the UV continuum spectrum was found to vary significantly, but the time scale of the UV variability remains to be determined by periodic observations. An outstanding question for QSOs with both a strong optical/UV bump and a soft

X-ray excess, of which H1821+643 is a prime example, is whether these components have a common origin. Simultaneous observations at UV and soft X-ray frequencies could determine whether both features are present at the same time. If both emissions arise in an accretion disk, then this should be reflected in the continuum energy distribution and the correlated variability of the UV and soft X-ray flux. To fit both the UV bump and the soft X-ray excess as one feature seems problematic in the current accretion disk models (e.g., requiring highly inclined disks around rapidly rotating holes, as shown by Sun & Malkan 1989a, or the inclusion of a strong Comptonized component, as calculated by Czerny & Elvis 1987). H1821+643, with its strong emission in all wavelength bands (except radio), and its variability in the UV and soft

X-ray flux, is an outstanding candidate for simultaneous monitoring in the X-ray and the UV band.

We acknowledge the able assistance of the staff at the Goddard *IUE* Regional Data Analysis Facility. We thank Martin Elvis and Saeqa Vrtilek for obtaining the infrared and optical magnitudes, respectively. This research was supported by NASA *IUE* grants NAG 5-1140 and NAG 5-1425 to the Columbia Astrophysics Laboratory. A. V. F. is supported by NASA grant NAG 5-1171, as well as by NSF grants AST-8957063 and AST-9003829. Lick Observatory is partially funded by NSF Core Block grant AST-8614510. This paper is contribution number 432 of the Columbia Astrophysics Laboratory.

REFERENCES

- Bechtold, J., Czerny, B., Elvis, M., Fabbiano, G., & Green, R. F. 1987, *ApJ*, 314, 699
- Begelman, M. C., Sikora, M., & Rees, M. J. 1987, *ApJ*, 313, 689
- Bergeron, J. 1988, in *QSO Absorption Lines*, ed. J. C. Blades, D. Turnshek, & C. A. Norman (Cambridge: Cambridge University Press), p. 127
- Bohlin, R. C., Savage, B. D., & Drake, J. F. 1978, *ApJ*, 224, 132
- Cunningham, C. T. 1975, *ApJ*, 202, 788
- Cutri, R. M., Wisniewski, W. Z., Rieke, G. H., & Lebofsky, M. J. 1985, *ApJ*, 296, 423
- Czerny, B., & Elvis, M. 1987, *ApJ*, 321, 305
- Edelson, R. A., Krolik, J. H., & Pike, G. F. 1990, *ApJ*, 359, 86
- Edelson, R. A., & Malkan, M. A. 1986, *ApJ*, 308, 59
- Elvis, M. 1988, in *Supermassive Black Holes*, ed. M. Kafatos (Cambridge: Cambridge University Press), p. 131
- Elvis, M., Wilkes, B. J., & McDowell, J. C. 1989, in *Extreme Ultraviolet Astronomy*, ed. R. F. Malina & S. Bowyer (New York: Pergamon)
- Filippenko, A. V. 1982, *ASP*, 94, 715
- Frank, J., King, A. R., & Raine, D. J. 1985, in *Accretion Power in Astrophysics* (Cambridge: Cambridge University Press), p. 101
- Grauer, A. D., & Bond, H. E. 1984, *ApJ*, 277, 211
- Kii, T., et al. 1991, in *ApJ*, in press.
- Kinney, A. L., Huggins, P. J., Bregman, J. N., & Glassgold, A. E. 1985, *ApJ*, 291, 128
- Kriss, G. A. 1988, *ApJ*, 324, 809
- Krolik, J. H., & Kallman, T. R. 1988, *ApJ*, 324, 714
- Kwan, J., & Krolik, J. H. 1981, *ApJ*, 250, 478
- Madau, P. 1988, *ApJ*, 327, 116
- Malkan, M. A., & Sargent, W. L. W. 1982, *ApJ*, 254, 22
- Marshall, F. E., Boldt, E. A., Holt, S. S., Mushotsky, R. F., Pravdo, S. H., Rothschild, R. E., & Serlemitsos, P. J. 1979, *ApJS*, 40, 657
- Massey, P., Strobel, K., Barnes, J. V., & Anderson, E. 1988, *ApJ*, 328, 315
- Miller, J. S., & Stone, R. P. S. 1987, the CCD Cassegrain Spectrograph at the Shane Reflector (Lick Observatory Technical Report No. 48, Santa Cruz, CA)
- Neugebauer, G., Miley, G. K., Soiffer, B. T., & Clegg, P. E. 1986, *ApJ*, 308, 815
- Nugent, J. J., et al. 1983, *ApJS*, 51, 1
- Oke, J. B., & Gunn, J. E. 1983, *ApJ*, 266, 713
- Pettini, M., et al. 1982, *MNRAS*, 199, 409
- Pravdo, S. H., & Marshall, F. E. 1984, *ApJ*, 281, 570
- Reichert, G. A., Polidan, R. S., Wu, C.-C., & Carone, T. E. 1988, *ApJ*, 325, 671
- Savage, B. D. 1988, in *QSO Absorption Lines*, ed. J. C. Blades, D. Turnshek, & C. A. Norman (Cambridge: Cambridge University Press), p. 195
- Scott, H. A., & O'Dell, S. L. 1989, in *IAU Symposium 134, Active Galactic Nuclei*, ed. D. E. Osterbrock & J. S. Miller (Dordrecht: Reidel), p. 257
- Seaton, M. J. 1979, *MNRAS*, 187, 73P
- Shakura, N. I., & Sunyaev, R. A. 1973, *A&A*, 24, 337
- Snyder, W. A., & Wood, K. S. 1984, in *X-ray and UV Emission from Active Galactic Nuclei*, ed. W. Brinkman & J. Truemper (Garching: Max Planck Institut), p. 114
- Stark, A. A., Heiles, C., Bally, J., & Linke, R. 1990, in preparation
- Sun, W.-H., & Malkan, M. A. 1987, in *Astrophysical Jets and Their Engines*, ed. W. Kundt (Dordrecht: Reidel), p. 125
- . 1989a, *ApJ*, 346, 68
- . 1989b, in *IAU Symposium 134, Active Galactic Nuclei*, ed. D. E. Osterbrock & J. S. Miller (Dordrecht: Reidel), p. 262
- Turner, M. J. L., et al. 1989, in *Proceedings of 23d ESLAB Symp.* (Noordwijk, The Netherlands: ESA Publ.), p. 769
- Wandel, A., & Petrosian, V. 1988, *ApJ*, 329, L11
- Warwick, R. S., Barstow, M. A., & Yaqoob, T. 1989, *MNRAS*, 238, 917
- Wills, B. J., Netzer, H., & Wills, D. 1985, *ApJ*, 288, 94
- Wood, K. S., et al. 1984, *ApJS*, 56, 507

THE REDSHIFT OF THE X-RAY SELECTED BL LACERTAE OBJECT H0414+009¹JULES P. HALPERN² AND VERA S. CHEN

Columbia Astrophysics Laboratory, Columbia University, 538 West 120th Street, New York, New York 10027

GREG M. MADEJSKI

Universities Space Research Association, and Laboratory for High Energy Astrophysics, NASA Goddard Space Flight Center, Code 666, Greenbelt, Maryland 20771

GARY A. CHANAN

Department of Physics, University of California, Irvine, California 92717

Received 6 September 1990; revised 30 October 1990

ABSTRACT

The x-ray selected BL Lac object H0414 + 004 has a redshift of 0.287, measured from the starlight of its host galaxy. The optical spectrum is well described by the sum of a standard elliptical galaxy plus a relatively flat power law ($\alpha \sim 0.3$). The galaxy contributes $\sim 40\%$ of the light in the spectrum in the rest-frame V band, and is one of the most luminous galaxies known ($M_V \sim -24$). The properties of H0414 + 009 are similar in all respects to a previously studied object, 1E 1415 + 259 at $z = 0.237$. If x-ray selected BL Lacs continue to be found in such bright galaxies, then the prospects of studying their luminosity function and evolution are considerably enhanced. There is also possible evidence for intrinsic x-ray absorption by a warm medium, as has been found in several other BL Lacs.

1. INTRODUCTION

The BL Lac object H0414 + 009 was first detected by the *HEAO 1* satellite, and identified in Einstein Observatory x-ray images. The original x-ray, optical, and radio observations were described by Ulmer *et al.* (1983). Further analysis of the Einstein observations was done by Madejski (1985), and subsequent *EXOSAT* x-ray observations were described by George (1988) and by Giommi *et al.* (1990). The polarization measurement by Impey & Tapia (1988) confirmed the BL Lac classification. The spectroscopy reported in this paper serves to demonstrate that there are no emission lines in the 1200–9000 Å range, and that the spectrum can be decomposed into starlight and power-law components. The measured redshift of 0.287, combined with the recent detection of the host galaxy by Falomo *et al.* (1990), makes this one of the most luminous BL Lacs, both in x-ray and starlight components.

2. OPTICAL SPECTROSCOPY

Spectra of H0414 + 009 were obtained with the UV Schmidt spectrograph on the Lick 3 m telescope on 1986 October 2. Two 3000 s exposures with different gratings were used to cover the spectral range 3150–9200 Å at a dispersion of 4 Å per pixel on a TI CCD. The slit width was 2".1, and the spectra were extracted from a 5".9 length along the slit. Standard stars of Oke & Gunn (1983), observed and reduced in the same manner, were used for flux calibration and removal of atmospheric absorption bands in the red region. It was found that the fluxes of the two spectra differed by 4% in the region of overlap, probably due to variable

seeing and/or guiding errors. Therefore, the flux of one spectrum was multiplied by a constant factor of 1.04 to produce the smooth composite spectrum shown in Fig. 1.

The redshift was derived from the weak stellar absorption features of Ca II, Mg b, and Na D, all of which agree with $z = 0.287 \pm 0.001$. Confirmation of the redshift was obtained with spectra taken on the 2.4 m Hiltner telescope of the Michigan–Dartmouth–MIT Observatory on 1989 November 8 and 9. Figure 2 shows the sum of six exposures totaling 3 hr, taken with the Mark III grism spectrograph and a Thomson CCD. The dispersion is 5 Å per pixel, and the slit width was 1".7. Data reduction procedures were the same as for the Lick spectra. In both spectra, the Na D line, redshifted to 7583 Å, is partly contaminated by the atmospheric A band, but its reality is not in doubt as its center lies 10 Å blueward of the band head.

Quite apart from the individual stellar absorption lines, the broadband shape of the spectrum is consistent with the sum of a power law and an elliptical galaxy at the measured redshift. Following the method of Halpern *et al.* (1986, hereafter referred to as Paper I), the composite Lick spectrum was fit by the sum of a power law of the form $f_\nu \propto \nu^{-\alpha}$, and the standard giant elliptical galaxy of Yee & Oke (1978). The data were first dereddened by $E_{B-V} = 0.15$, corresponding to the neutral hydrogen column density of $9 \times 10^{20} \text{ cm}^{-2}$ measured toward this object by Elvis *et al.* (1989). The results of this decomposition are shown in Fig. 3, and are strikingly similar to the analysis of the spectrum of 1E 1415 + 259 in Paper I. The best fit corresponds to a starlight fraction of 0.40 at the rest wavelength of 5460 Å. At 4000 Å, the starlight fraction is only 0.19. The power-law component is rather flat, $\alpha \sim 0.3$, but consistent with that in 1E 1415 + 259 and other x-ray selected BL Lacs. It is not possible to determine α with high precision due to a number of uncertainties, including the real shape of the underlying galaxy continuum and likely errors in spectrophotometry over

¹ Based on observations obtained at Lick Observatory, operated by the University of California, and at the Michigan–Dartmouth–MIT Observatory.

² Guest Observer with the *International Ultraviolet Explorer Satellite*.

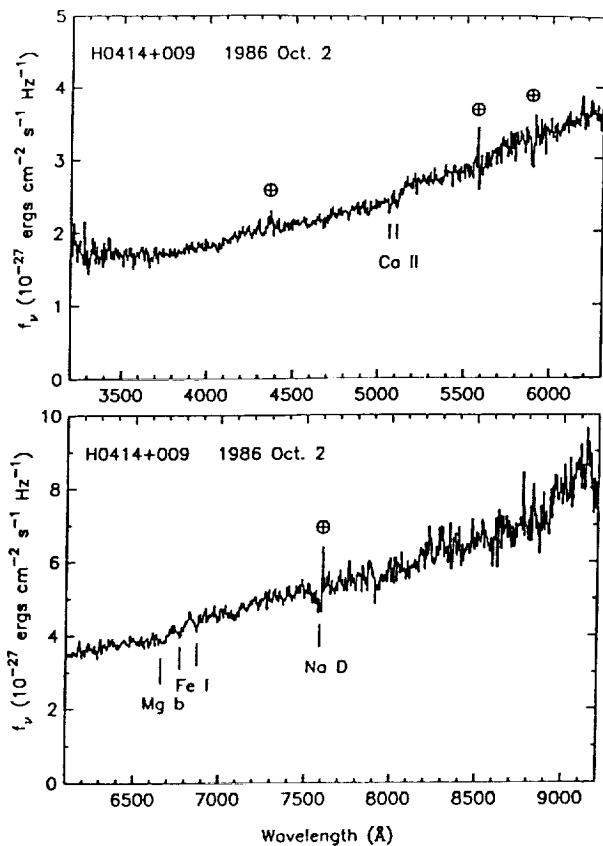


FIG. 1. Spectrum of H0414 + 009 obtained at Lick Observatory. Stellar absorption lines at $z = 0.287$ are indicated (tick marks), as are spurious features due to imprecise removal of emission and absorption features of terrestrial origin (\oplus).

the wide wavelength range. For example, the fit deviates from the data by as much as 10% at the ends of the spectrum no matter what decomposition is tried. An uncertainty of at least ± 0.3 in α must be allowed.

3. ULTRAVIOLET AND X-RAY OBSERVATIONS

A 350 min exposure of H0414 + 009 was obtained with *IUE* on 1986 December 22 using the large aperture of the

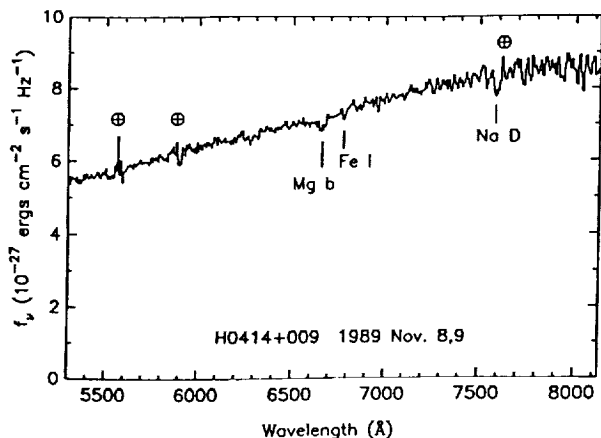


FIG. 2. Spectrum of H0414 + 009 obtained on the Hiltner telescope of the MDM Observatory. The redshift of 0.287 is consistent with that obtained at Lick.

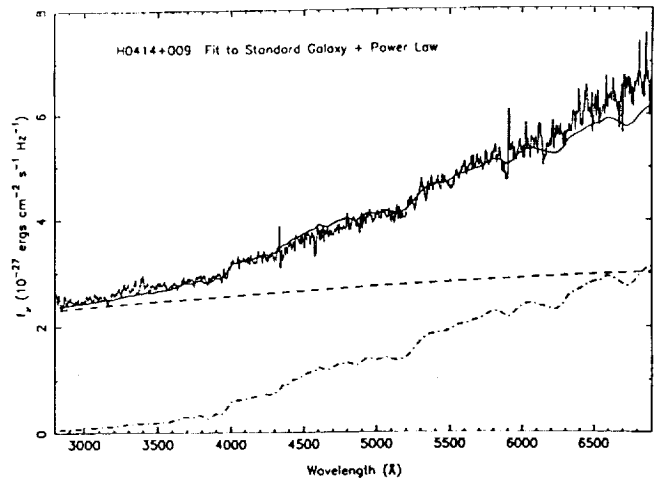


FIG. 3. The best fit (solid line) for a decomposition of the Lick Observatory spectrum into a power law (dashed line) plus standard giant elliptical galaxy (dot-dash line). The power law is $\nu^{-\alpha}$. The data were corrected for $E_B - V = 0.15$ in our Galaxy, estimated from the neutral hydrogen column density toward H0414 + 009.

SWP camera. The continuum was detected only weakly, and therefore is heavily contaminated with camera artifacts (Crenshaw *et al.* 1990). A rough estimate of the flux in the 1500 Å region is $\sim 1 \times 10^{-27}$ ergs $\text{cm}^{-2} \text{s}^{-1} \text{Hz}^{-1}$, or $\sim 3 \times 10^{-27}$ ergs $\text{cm}^{-2} \text{s}^{-1} \text{Hz}^{-1}$ after dereddening by $E_B - V = 0.15$. Two LWP spectra were obtained in 1987 March by George (1988), and are similarly weak. The mean flux in the 2600–3100 Å band derived by George is $\sim 2.5 \times 10^{-27}$. These flux levels are very similar to that of the power-law component in the optical, and would be indicative of a flat energy distribution between the UV and the optical if it were not for the large uncertainties in the spectrophotometry and the nonsimultaneity of the observations.

Of the x-ray observations mentioned in Sec. 1, the Einstein data obtained simultaneously by the imaging proportional counter (IPC) and the monitor proportional counter (MPC) (Ulmer *et al.* 1983) can now be fit jointly to obtain spectral parameters that are more accurate than were previously obtained from each instrument separately. A fit to a standard power-law continuum with absorption yields energy index $\alpha = 1.6 (+0.5, -0.4)$ and column density $N_H = 3.5 (+1.8, -1.4) \times 10^{21} \text{ cm}^{-2}$. The errors are 90% confidence for the two parameters. The χ^2 is 12.5 for 16 deg of freedom. The x-ray flux in the 2–6 keV band is 1.9×10^{-11} ergs $\text{cm}^{-2} \text{s}^{-1}$. Another Einstein MPC observation during which the high resolution imager was in the focal plane, yielded similar although somewhat less restrictive spectral parameters.

The most surprising result of the x-ray spectral fit is the rather high hydrogen column density, which is at least 2.3 times larger than the Galactic 21 cm value of 9×10^{20} measured toward the object. There are several reasons to suspect that this extra absorption is intrinsic to the BL Lac object, and that it is due to highly ionized gas. First, it is very unlikely that the true reddening is three times the Galactic value, since this would make the corrected ultraviolet flux greater than the optical, a situation which is never seen in BL Lac objects. Therefore, the origin of the extra absorption must not be in ordinary cold interstellar material. Second, the

EXOSAT spectra of H0414 + 009 derived from joint fits to the low-energy and medium-energy detectors yielded $N_{\text{H}} = 1.2 \pm 0.2 \times 10^{21}$ (George 1988), which is much closer to the Galactic value. This can be understood if the absorbing material is highly ionized. Since the *EXOSAT* low-energy detector is sensitive to lower-energy x-rays than is the Einstein IPC, it could detect flux below the oxygen K-edge which would be unabsorbed if the hydrogen and helium were totally ionized. Third, there are other BL Lac objects, which have been observed with the higher resolution x-ray spectrometers on Einstein, whose x-ray spectra are consistent with an absorption trough of highly ionized oxygen. The prototype is PKS 2155-304 (Canizares & Kruper 1984), and there are several others (Urry *et al.* 1986; Madejski *et al.* 1990).

For these reasons, the "standard" x-ray spectral fit involving only a neutral absorber is probably not an appropriate model. Although the IPC cannot directly resolve an absorption trough of ionized oxygen, it seems reasonable that the presence of this extra feature would be consistent with all the available data on H0414 + 009. Fits to the IPC/MPC data which include an absorption line centered between 0.5 and 0.6 keV give equally good χ^2 values as the "standard" model, if the equivalent width of the line is about 0.5 keV. Future high-resolution x-ray spectroscopy will be necessary to establish whether an ionized absorber is present in H0414 + 009, and in x-ray bright BL Lacs in general.

4. DISCUSSION AND CONCLUSIONS

The redshift of 0.287 makes this one of the most luminous BL Lacs in x rays, since the 2–6 keV flux of 1.9×10^{-11} ergs cm⁻² s⁻¹ corresponds to a luminosity of 1.0×10^{46} ergs s⁻¹ (for $H_0 = 50$ km s⁻¹ Mpc⁻¹, $q_0 = 0$) in the intrinsic 2–6 keV energy band. The host galaxy is also very bright, probably accounting for about half the light in the *R* band (corresponding to the *V* band in the rest frame of the galaxy). Falomo *et al.* (1990) recently imaged the host galaxy, detecting it out to at least 3.5 from the nucleus. Their *R* magnitude of 16.6 is in good agreement with the values of 17.0 and 16.4 which can be estimated from the Lick and Hiltner spectra, respectively. Therefore, the galaxy contribution can be estimated as $m_R \sim 17.3$ (half the flux in the *R* band), and the equivalent absolute magnitude in the *V* band is $M_V \sim -24$. Following the discussion in Paper I, this is 1 mag brighter than the first-ranked cluster ellipticals, and similar to the host galaxy of 1E 1415 + 259.

In Paper I, it was concluded on the basis of surface pho-

tometry that the host galaxy of 1E 1415 + 259 is better described as an exponential disk than an elliptical, although all other BL Lac hosts are better fit by an elliptical $r^{1/4}$ law (Ulrich 1989). We do not know what the profile of the host galaxy of H0414 + 009 is like, but it is obviously an important candidate for further deep imaging at high spatial resolution. Imaging in the *I* band would further reduce the relative contribution of the active nucleus. In all other respects, these two luminous BL Lacs are very similar. Their continuum energy distributions from radio through x-rays scale almost exactly.

Gravitational microlensing of OVV quasars by stars in a foreground galaxy has been suggested as an alternative model for BL Lac objects (Ostriker & Vietri 1985, 1990). This scenario would be rendered plausible if the BL Lac were displaced from the center of the galaxy. Although displacements have been suggested in several objects, we see no evidence for misalignment in either H0414 + 009 or 1E 1415 + 259. A more conventional theory would instead try to connect the extreme luminosity of the host galaxy to the BL Lac properties.

The prospects of studying the luminosity function and evolution of BL Lacs (e.g., Wolter *et al.* 1989) will be enhanced considerably if x-ray selected members continue to be found in such luminous galaxies. X-ray selection is the best method of obtaining a complete sample of BL Lac objects, and the *ROSAT* all sky x-ray survey is likely to detect several hundred. This method of finding the redshift from the starlight contribution to the spectrum could be extended to $z \sim 1$ by using the Ca II H and K feature, which is associated with a sharp discontinuity in the spectrum in addition to its narrow absorption lines. Of course, this method will succeed only if the relative contributions of the starlight and nonthermal components are such that the break can be measured. Alternatively, the redshift might be obtained from the off-nuclear light under conditions of good seeing. And finally, these objects will be prime targets for the study of host galaxies of BL Lacs using the *Hubble Space Telescope*.

We are grateful to Greg Bothun for making time available on the Hiltner telescope and for his assistance, even though he pretended to frown on this particular observation. The x-ray data were obtained from the Einstein Data Bank, with the help of John McSweeney. This is contribution number 433 of the Columbia Astrophysics Laboratory, and was supported by NASA Grant Nos. NAG 8-497 and NAG 5-1425.

REFERENCES

- Canizares, C. R., and Kruper, J. 1984, *ApJ*, 278, L99
 Crenshaw, D. M., Bruegman, O. W., and Norman, D. J. 1990, *PASP*, 102, 463
 Elvis, M., Lockman, F. J., and Wilkes, B. J. 1989, *AJ*, 97, 777
 Falomo, R., Melnick, J., and Tanzi, E. G. 1990, *Nat*, 345, 692
 George, I. 1988, Ph.D. thesis, University of Leicester
 Giommi, P., Barr, P., Garilli, B., Maccagni, D., and Pollock, A. M. T. 1990, *ApJ*, 356, 432
 Halpern, J. P., Impey, C. D., Bothun, C. D., Tapia, S., Skillman, E. D., Wilson, A. S., and Meurs, E. J. A. 1986, *ApJ*, 302, 711
 Impey, C. D., and Tapia, S. 1988, *ApJ*, 333, 666
 Madejski, G. M. 1985, Ph.D. thesis, Harvard University
 Madejski, G. M., Mushotzky, R. F., Weaver, K. A., Arnaud, K. A., and Urry, C. M. 1990, *ApJ*, (in press)
 Oke, J. B., and Gunn, J. E. 1983, *ApJ*, 266, 713
 Ostriker, J. P., and Vietri, M. 1985, *Nat*, 318, 446
 Ostriker, J. P., and Vietri, M. 1990, *Nat*, 344, 45
 Ulmer, M. P., Brown, R. L., Schwartz, D. A., Patterson, J., and Cruddace, R. G. 1983, *ApJL*, 270, L1
 Ulrich, M.-H. 1989, in *BL Lac Objects*, edited by L. Maraschi, M. Maccacaro, and M.-H. Ulrich (Springer, Berlin), p. 45
 Urry, C. M., Mushotzky, R. F., and Holt, S. S. 1986, *ApJ*, 305, 369
 Wolter, A., Gioia, I. M., Maccacaro, T., Schild, R. E., Morris, S. L., and Stocke, J. T. 1989, in *Proceedings of the 23rd ESLAB Symposium, Two Topics in X-Ray Astronomy*, edited by J. Hunt and B. Batrick (ESA, Noordwijk), p. 749
 Yee, H. C., and Oke, J. B. 1978, *ApJ*, 226, 753